

Differential learning methods for solving fully nonlinear PDEs

William LEFEBVRE* Grégoire LOEPER† Huyên PHAM ‡

May 23, 2022

Abstract

We propose machine learning methods for solving fully nonlinear partial differential equations (PDEs) with convex Hamiltonian. Our algorithms are conducted in two steps. First the PDE is rewritten in its dual stochastic control representation form, and the corresponding optimal feedback control is estimated using a neural network. Next, three different methods are presented to approximate the associated value function, i.e., the solution of the initial PDE, on the entire space-time domain of interest. The proposed deep learning algorithms rely on various loss functions obtained either from regression or pathwise versions of the martingale representation and its differential relation, and compute simultaneously the solution and its derivatives. Compared to existing methods, the addition of a differential loss function associated to the gradient, and augmented training sets with Malliavin derivatives of the forward process, yields a better estimation of the PDE's solution derivatives, in particular of the second derivative, which is usually difficult to approximate. Furthermore, we leverage our methods to design algorithms for solving families of PDEs when varying terminal condition (e.g. option payoff in the context of mathematical finance) by means of the class of DeepOnet neural networks aiming to approximate functional operators. Numerical tests illustrate the accuracy of our methods on the resolution of a fully nonlinear PDE associated to the pricing of options with linear market impact, and on the Merton portfolio selection problem.

Key words: Fully nonlinear PDEs, deep learning, differential learning, option pricing with market impact.

*BNP Paribas Global Markets, Université Paris Cité and Sorbonne Université, Laboratoire de Probabilités, Statistique et Modélisation (LPSM, UMR CNRS 8001), Building Sophie Germain, Avenue de France, 75013 Paris, [wlefebvre at lpsm.paris](mailto:wlefebvre@lpsm.paris)

†BNP Paribas Global Markets, School of Mathematics, Monash University, Clayton Campus, VIC, 3800, Australia, [gregoire.loeper at monash.edu](mailto:gregoire.loeper@monash.edu)

‡Université Paris Cité and Sorbonne Université, Laboratoire de Probabilités, Statistique et Modélisation (LPSM, UMR CNRS 8001), Building Sophie Germain, Avenue de France, 75013 Paris, [pham at lpsm.paris](mailto:pham@lpsm.paris)

1 Introduction

This paper is devoted to the resolution of fully nonlinear partial differential equations (PDEs) of the form

$$\begin{cases} \partial_t u + H(x, D_x u, D_x^2 u) = 0, & (t, x) \in [0, T) \times \mathbb{R}^d, \\ u(T, x) = g(x), & x \in \mathbb{R}^d, \end{cases} \quad (1.1)$$

where the Hamiltonian $H : \mathbb{R}^d \times \mathbb{R}^d \times \mathbb{R}^{d \times d} \rightarrow \mathbb{R} \cup \{\infty\}$ is a lower semi-continuous convex function with respect to the two last arguments (z, γ) , and g a measurable function on \mathbb{R}^d . The numerical resolution of this class of PDE is a notorious challenging problem, and it is especially difficult to obtain a good approximation of the second spatial derivative $D_x^2 u$ of the solution in this fully nonlinear context. In the last years, significant progress has been achieved towards these challenges with several numerical methods using techniques from deep learning, see the recent surveys by [3] and [8]: A first class of approximation algorithms, called *Physics Informed Neural Network* (PINNs) [28], also known as *Deep Galerkin method* (DGM) [30], directly approximates the solution to the PDE by a neural network, and its partial derivatives by automatic differentiation, by minimizing the loss function arising from the residual of the PDE evaluated on a random grid in the space-time domain. A second class of algorithms relies on the backward stochastic differential representation of the PDE in the semi-linear case by minimizing either a global loss function (see [6], and extensions in [2], [17], [24]), or sequence of loss functions from backward recursion (see [16], and variations-extensions in [25], [1], [8]).

In this article, we consider numerical methods for fully nonlinear PDEs based on machine learning techniques that are conducted in two steps. The starting point of our approach is to rewrite the PDE (1.1) with convex Hamiltonian in its stochastic control representation form following the duality arguments of [31]. An approximation of the associated optimal feedback control is then obtained using a neural network by a global optimization, as described in [12] and [11]. Based on this control approximation, two main approaches using neural networks are then developed in order to approximate the value function, hence the solution of the initial PDE on the space-time domain, which is formulated as a conditional expectation with respect to the approximate optimal state process.

The first one, called *Differential regression learning*, is inspired by [14]. In this paper, the authors compute conditional expectations of an option payoff in the spirit of the Longstaff-Schwartz method [19], by parametrizing it with a neural network and performing the regression simultaneously on the value and on the derivative of this neural network. The addition of a regression loss on the derivative, where the derivative of the network, computed by automatic differentiation, is regressed against the pathwise derivative of the conditional expectation integrand, improves the estimation of the first derivative of the conditional expectation and empirically speeds up the training by allowing to train the

network on smaller batches. We adapt this method to our context. Indeed, having approximated the optimal control of the stochastic control problem associated to the PDE, the associated value function can be expressed as the conditional expectation of a running payoff of optimally controlled state trajectories, while its gradient is represented also as a conditional expectation formula by differentiation of the payoff. This representation formulae provide two loss functions that will be minimized alternately in order to learn by neural network approximation both the solution of the PDE and its gradient.

The second approach, called Pathwise learning, is inspired by [34], where the authors compute the conditional expectation of a payoff by using the Feynman-Kac formula to derive a pathwise control variate corresponding to the hedging strategy. In their work, the derivative of the conditional expectation value, present in the hedging integral, is approximated by a neural network and optimized so as to minimize the variance of the conditional expectation estimator. This approach is analogous to the one derived in [26], with the addition of machine learning techniques. In our case, given the approximation of the stochastic control associated to the PDE, a martingale representation of the payoff is derived on optimally controlled trajectories. Our first pathwise method, called *Pathwise martingale learning*, uses this martingale representation to train the value and the first derivative of a neural network. This method is also in the spirit of the deep BSDE method of [3], but the minimization of our loss function provides directly an approximation of the solution and its gradient on the space-time domain. Our second method, called *Pathwise differential learning*, considers furthermore the derivative of this martingale representation, computed by automatic differentiation, which gives another loss function to be minimized in order to train neural networks for approximating the value function and its first and second derivatives. Such differential representation has been also considered in the recent paper [22] for designing a deep learning scheme with one-step loss functions as in the deep backward approach in [16] for solving forward backward SDEs with new estimation and error control of the Z process. Actually, the addition of this derivative loss function permits a better approximation of the terminal condition of the PDE and improves the overall approximation of the PDE solution's value and derivatives on the entire domain.

Finally, we leverage our deep learning algorithms for solving families of PDEs when varying the terminal condition. In other words, the input is a function g_K with parameter K , and the output is the solution to the PDE with terminal condition g_K . This is performed by means of the class of DeepOnet neural networks aiming to approximate functional operators. These networks, introduced in [20], rely on a universal approximation theorem for operators [5] stating that a neural network with a single hidden layer can approximate accurately any nonlinear continuous operator. The DeepOnet realizes this theorem in practice and can be used to learn the mapping between the terminal function of a PDE and its solution.

The outline of the paper is organized as follows. In Section 2, we present the problem, recall the dual stochastic control representation of fully nonlinear PDEs and outlines the different methods. In Section 3, we present the theory of the Differential regression learning

method, give the expression of the losses used to train the neural network and present the advantages of adding a loss to train the first derivative of the neural network. In Section 4, the Pathwise and Pathwise differential methods are developed and the expressions of the losses used to train the neural network are given. In Section 5, the implementation details and pseudo-codes of the different algorithms are presented along with validation tests and numerical results of the three methods on the Merton portfolio selection problem and on the Black-Scholes with linear market impact PDE. Finally, Section 6 presents a method to solve nonlinear parabolic PDEs with parametric terminal condition g_K for parameter values K in a compact set. The codes of our algorithms are available on <https://colab.research.google.com/drive/1xyE1U3SqN4Hjia2d3p0sCXCCDGWRUqsh?usp=sharing>.

Notations. We end this introduction with some notations that will be used in the sequel of the paper. The scalar product between two vectors b and z is denoted by $b \cdot z$, and $|\cdot|$ is the Euclidian norm. Given two matrices $A = (A_{ij})$ and $B = (B_{ij})$, we denote by $A : B = \text{Tr}(A^\top B) = \sum_{i,j} A_{ij} B_{ij}$ its inner product, and by $|A|$ the Frobenius norm of A . Here \top is the transpose matrix operator. \mathbb{S}^d is the set of $d \times d$ symmetric matrices with real coefficients equipped with the partial order: $\gamma_1 \leq \gamma_2$ iff $\gamma_2 - \gamma_1 \in \mathbb{S}_+^d$, the set of positive semidefinite matrices in \mathbb{S}^d .

Let $\mathbf{M} = (M_{i_1 i_2 i_3}) \in \mathbb{R}^{d_1 \times d_2 \times d_3}$ be a tensor of order 3. For $p = 1, 2, 3$, the p -mode product of \mathbf{M} with a vector $b = (b_i) \in \mathbb{R}^{d_p}$, is denoted by $\mathbf{M} \bullet_p b$, and it is a tensor of order 2, i.e. a matrix defined elementwise as

$$(\mathbf{M} \bullet_1 b)_{i_2 i_3} = \sum_{i_1=1}^{d_1} M_{i_1 i_2 i_3} b_{i_1}, \quad (\mathbf{M} \bullet_2 b)_{i_1 i_3} = \sum_{i_2=1}^{d_2} M_{i_1 i_2 i_3} b_{i_2}, \quad (\mathbf{M} \bullet_3 b)_{i_1 i_2} = \sum_{i_3=1}^{d_3} M_{i_1 i_2 i_3} b_{i_3}$$

The p -mode product of a 3-th order tensor $\mathbf{M} \in \mathbb{R}^{d_1 \times d_2 \times d_3}$ with a matrix $B = (B_{ij}) \in \mathbb{R}^{d_p \times d}$, also denoted by $\mathbf{M} \bullet_p B$, is a 3-th order tensor defined elementwise as

$$\begin{aligned} (\mathbf{M} \bullet_1 B)_{\ell i_2 i_3} &= \sum_{i_1=1}^{d_1} M_{i_1 i_2 i_3} B_{i_1 \ell}, & (\mathbf{M} \bullet_2 B)_{i_1 \ell i_3} &= \sum_{i_2=1}^{d_2} M_{i_1 i_2 i_3} B_{i_2 \ell} \\ (\mathbf{M} \bullet_3 B)_{i_1 i_2 \ell} &= \sum_{i_3=1}^{d_3} M_{i_1 i_2 i_3} B_{i_3 \ell}. \end{aligned}$$

Finally, the tensor contraction (or partial trace) of a 3-th order tensor $\mathbf{M} \in \mathbb{R}^{d_1 \times d_2 \times d_3}$ whose dimensions d_p and d_q are equal is denoted as $\text{Tr}_{p,q} \mathbf{M}$. This tensor contraction is a tensor of order 1, i.e. a vector, defined elementwise as

$$(\text{Tr}_{1,2} \mathbf{M})_{i_3} = \sum_{\ell=1}^{d_1} M_{\ell i_3}, \quad (\text{Tr}_{1,3} \mathbf{M})_{i_2} = \sum_{\ell=1}^{d_1} M_{\ell i_2}, \quad (\text{Tr}_{2,3} \mathbf{M})_{i_1} = \sum_{\ell=1}^{d_2} M_{i_1 \ell}.$$

2 Dual stochastic control representation of fully nonlinear PDE

We consider a fully nonlinear partial differential equation (PDE) of parabolic type:

$$\begin{cases} \partial_t u + H(x, D_x u, D_x^2 u) = 0, & (t, x) \in [0, T] \times \mathbb{R}^d, \\ u(T, x) = g(x), & x \in \mathbb{R}^d, \end{cases} \quad (2.1)$$

where the Hamiltonian $H : \mathbb{R}^d \times \mathbb{R}^d \times \mathbb{R}^{d \times d} \rightarrow \mathbb{R} \cup \{\infty\}$ is a lower semi-continuous convex function w.r.t the two last arguments (z, γ) , and g a measurable function on \mathbb{R}^d . As it is usual, we assume that $H(x, z, \gamma) = H(x, z, \gamma^\top)$, and that $\gamma \in \mathbb{S}^d \mapsto H(x, z, \gamma)$ is nondecreasing,

Without loss of generality, we may then assume that H is in a Bellman form:

$$H(x, z, \gamma) = \sup_{a \in A} [b(x, a) \cdot z + \frac{1}{2} \sigma \sigma^\top(x, a) : \gamma + f(x, a)], \quad (x, z, \gamma) \in \mathbb{R}^d \times \mathbb{R}^d \times \mathbb{S}^d, \quad (2.2)$$

for some measurable functions $b : \mathbb{R}^d \times A \rightarrow \mathbb{R}^d$, $\sigma : \mathbb{R}^d \times A \rightarrow \mathbb{R}^{d \times m}$, $f : \mathbb{R}^d \times A \rightarrow \mathbb{R}$, and with A some subset of \mathbb{R}^q . Indeed, such form may arise directly from the dynamic programming equation of a stochastic control problem. Otherwise, it can be written in this formulation by following the duality argument as in [31]. We introduce the concave conjugate of the function $H(x, z, \gamma)$ w.r.t. the last two variables, i.e.

$$f(x, b, c) := \inf_{z \in \mathbb{R}^d, \gamma \in \mathbb{R}^{d \times d}} [H(x, z, \gamma) - b \cdot z - \frac{1}{2} c : \gamma], \quad x \in \mathbb{R}^d, b \in \mathbb{R}^d, c \in \mathbb{R}^{d \times d},$$

and notice that $f(x, b, c) = f(x, b, c^\top)$ as $H(x, z, \gamma) = H(x, z, \gamma^\top)$. By the Fenchel-Moreau duality relation, we then get

$$\begin{aligned} H(x, z, \gamma) &= \sup_{b \in \mathbb{R}^d, c \in \mathbb{S}^d} [b \cdot z + \frac{1}{2} c : \gamma + f(x, b, c)] \\ &= \sup_{(b, c) \in D_f} [b \cdot z + \frac{1}{2} c : \gamma + f(x, b, c)], \quad \text{for } x \in \mathbb{R}^d, z \in \mathbb{R}^d, \gamma \in \mathbb{S}^d, \end{aligned}$$

where $D_f := \{(b, c) \in \mathbb{R}^d \times \mathbb{S}^d : f(x, b, c) > -\infty\} \subset \mathbb{R}^d \times \mathbb{S}_+^d$ by the nondecreasing monotonicity of $\gamma \mapsto H(x, z, \gamma)$. By assuming that H is uniformly continuous in x , we notice that the domain D_f does not depend on x . Since for any $c \in \mathbb{S}_+^d$, there exists a unique $s \in \mathbb{S}_+^d$ s.t. $c = s^2$, the above duality relation is in the Bellman form (2.2) with $a = (b, s) \in A = \{(b, s) \in \mathbb{R}^d \times \mathbb{S}_+^d : f(x, b, s^2) > -\infty\}$, $b(x, a) = b$, $\sigma(x, a) = s$, $f(x, a) = f(x, b, s^2)$.

It is well-known that the solution to the PDE (2.1) with an Hamiltonian H as in (2.2) admits the stochastic representation:

$$u(t, x) = \sup_{\alpha \in \mathcal{A}} \mathbb{E} \left[g(X_T^{t, x, \alpha}) + \int_t^T f(X_s^{t, x, \alpha}, \alpha_s) ds \right], \quad (t, x) \in [0, T] \times \mathbb{R}^d, \quad (2.3)$$

where $X = X^{t,x,\alpha}$ is solution to the stochastic differential equation

$$dX_s = b(X_s, \alpha_s)ds + \sigma(X_s, \alpha_s)dW_s, \quad t \leq s \leq T, \quad X_t = x, \quad (2.4)$$

on a filtered probability space $(\Omega, \mathcal{F}, \mathbb{F} = (\mathcal{F}_t)_{0 \leq t \leq T}, \mathbb{P})$ along with a m -dimensional Brownian motion W , and the control $\alpha \in \mathcal{A}$ is a pair of \mathbb{F} -progressively measurable processes valued in A , satisfying suitable integrability conditions for ensuring under some Lipschitz assumptions on the coefficients b, σ that the SDE (2.4) admits a unique strong solution.

Problem (2.3) is a standard stochastic control problem with controlled Markov state process X governed by (2.4), and it is well-known that when it exists the optimal control $\hat{\alpha} \in \mathcal{A}$ is in closed-loop (or feedback) form, i.e.

$$\hat{\alpha}_s = \hat{a}(s, \hat{X}_s^{t,x}), \quad t \leq s \leq T, \quad (t, x) \in [0, T] \times \mathbb{R}^d,$$

for some measurable function $\hat{a} : [0, T] \times \mathbb{R}^d \rightarrow A \subset \mathbb{R}^q$, where \hat{X} is the state process controlled by $\hat{\alpha}$. From the time-consistency of the stochastic control problem (2.3), we notice that this feedback form \hat{a} does not depend on the starting point $(t, x) \in [0, T] \times \mathbb{R}^d$ of the value function. Furthermore, the value function u is given by the conditional expectation

$$u(t, x) = \mathbb{E} \left[g(\hat{X}_T) + \int_t^T f(\hat{X}_s, \hat{a}(s, \hat{X}_s)) ds \mid \hat{X}_t = x \right]. \quad (2.5)$$

Our resolution method for approximating a solution to (2.1) on the whole domain $[0, T] \times \mathbb{R}^d$ is performed in two steps:

1. First, following the deep learning approach in [12], we shall use neural networks functions $a_\theta : [0, T] \times \mathbb{R}^d \rightarrow A \subset \mathbb{R}^q$, to approximate the optimal feedback control \hat{b} , by maximizing over parameters θ the objective function

$$J(\theta) = \mathbb{E} \left[g(X_T^\theta) + \int_0^T f(X_t^\theta, a_\theta(t, X_t^\theta)) dt \right], \quad (2.6)$$

where X^θ solves

$$dX_t^\theta = b(X_t^\theta, a_\theta(t, X_t^\theta))dt + \sigma(X_t^\theta, a_\theta(t, X_t^\theta))dW_t, \quad 0 \leq t \leq T,$$

with initial condition X_0^θ distributed according to some law μ_0 on \mathbb{R}^d . We denote by θ^* the “optimal parameter” that maximizes $J(\theta)$, and set $a^* = a_{\theta^*}$. We denote by $X^* = X^{\theta^*}$ an approximation of the optimal state process \hat{X} . For the numerical implementation, we discretize in time the process X^θ and the integral over f in (2.6), and apply a stochastic gradient ascent algorithm based on samples of X^θ . The pseudo-code is presented in Algorithm 1.

2. Once we get an approximation of the optimal feedback control, we could in principle compute $u(t, x)$ from the Feynman-Kac representation (2.5) by Monte-Carlo simulations of X^* . However, with the purpose of solving the PDE (2.1) on the whole domain, this has to be performed for every point $(t, x) \in [0, T] \times \mathbb{R}^d$, which is not feasible in practice. Instead, we apply three types of differential learning methods for approximating simultaneously the value function u , as well as its derivative: (i) the first one, called *differential regression learning*, is directly inspired from the original approach in [14], and gives an approximation of u and its first derivative $D_x u$ from the minimization of two loss functions based on least-square regressions, (ii) the second one in the spirit of [26], [34], which uses a contingent claim hedging strategy as a Monte Carlo control variate, approximates the value function and its first derivative from the minimization of a single loss function based on the martingale representation in (2.5), and is referred to as *pathwise martingale learning* method. (iii) the third one, called *pathwise differential learning*, provides in addition an accurate approximation of the second derivative $D_x^2 u$ of u . We develop these three methods and present their pseudo-codes in the next sections.

Notice that since the neural network a^* is by nature a suboptimal feedback policy, the approximation computed in the second step provides a lower bound for the value function u solution to the PDE.

3 Differential regression learning

From the conditional expectation representation (2.5), and its fundamental characterization property as an L^2 -regression, we have

$$u(t, \hat{X}_t) = \arg \min_{v_t} \mathbb{E} |\hat{Y}_T^t - v_t(\hat{X}_t)|^2(\hat{X}_t), \quad \text{for all } t \in [0, T],$$

where the target payoff is

$$\hat{Y}_T^t = g(\hat{X}_T) + \int_t^T f(\hat{X}_s, \hat{a}(s, \hat{X}_s)) ds, \quad t \in [0, T], \quad (3.1)$$

and the argmin is taken over measurable real-valued functions v_t on \mathbb{R}^d s.t. $v_t(\hat{X}_t)$ is square-integrable.

This suggests to use a class of neural networks (NN) functions ϑ^η on $[0, T] \times \mathbb{R}^d$, with parameters η , for approximating the value function u , and a loss function

$$\begin{aligned} \hat{L}_{val}(\eta) &= \mathbb{E} \left[\int_0^T |\hat{Y}_T^t - \vartheta^\eta(t, \hat{X}_t)|^2 dt \right] \\ &\simeq \mathbb{E} \left[\int_0^T |Y_T^{*,t} - \vartheta^\eta(t, X_t^*)|^2 dt \right] =: L_{val}^*(\eta), \end{aligned} \quad (3.2)$$

where

$$Y_T^{*,t} = g(X_T^*) + \int_t^T f(X_s^*, a^*(s, X_s^*)) ds, \quad t \in [0, T].$$

As pointed out in [14], the training of the loss function L_{val}^* in (3.2) would require a vast number of samples (often of order millions) to learn accurate approximation of the value function, and is furthermore prone to overfitting. Indeed, by training a neural network to minimize L_{val}^* , we would obtain a function which interpolates the random points generated during training. This comes with two shortcomings. First, a large number of training samples is needed to get satisfactory values of the solution and a good enough generalisation to untrained domains. Second, the functions obtained by this method are usually noisy. If we are interested in the derivatives of the PDE solution, as it is the case in finance for example, where *greeks* are computed in order to hedge contingent claims, the solution computed might not be accurate enough. Some standard methods, such as Ridge and Lasso penalisations allow to reduce overfitting but come at the cost of adding bias and an arbitrary penalty and do not ensure that the derivative of the network will be a good approximation of the derivative of the PDE solution. To circumvent these issues, and following the idea in [14], we propose to consider furthermore the learning of the derivative of the value function. This method relies on pathwise differentiation of the target payoff \hat{Y}_T^t for deriving the gradient of the value function (see Chapter 7 in [9]):

$$D_x u(t, \hat{X}_t) = \mathbb{E} \left[\hat{Z}_T^t | \mathcal{F}_t \right], \quad t \in [0, T], \quad (3.3)$$

where $\hat{Z}_T^t = D_{\hat{X}_t} \hat{Y}_T^t$. This suggests to complete the learning of the value function together with its derivative by considering furthermore the loss function

$$\begin{aligned} \hat{L}_{der}(\eta) &= \mathbb{E} \left[\int_0^T |\hat{Z}_T^t - D_x \vartheta^\eta(t, \hat{X}_t)|^2 dt \right] \\ &\simeq \mathbb{E} \left[\int_0^T |Z_T^{*,t} - D_x \vartheta^\eta(t, X_t^*)|^2 dt \right] =: L_{der}^*(\eta), \end{aligned}$$

where $Z_T^{*,t} = D_{X_t^*} Y_T^{*,t}$ valued in \mathbb{R}^d , is obtained by automatic differentiation as

$$Z_T^{*,t} = (D_{X_t} X_T)^\top D_x g(X_T) + \int_t^T (D_{X_t} X_s)^\top D_x f^{a^*}(s, X_s) ds, \quad t \in [0, T], \quad (3.4)$$

where we denote by $f^{a^*}(t, x) = f(x, a^*(t, x))$, and assuming that g and f are continuously differentiable. Notice that $D_x f^{a^*} = D_x f + (D_x a^*)^\top D_a f$, where the derivatives $D_x a^*$ of the approximate optimal feedback control in the class of neural networks can be efficiently computed by automatic differentiation. Here, to alleviate notations, we have dropped the superscript $*$ for the state $X = X^*$. Actually, when g and f are only piecewise-differentiable,

the above relation still holds when the marginal law of X_s is absolutely continuous with respect to Lebesgue measure on \mathbb{R}^d , which is satisfied under nondegeneracy conditions on the diffusion coefficients (see Theorem 2.3.2 in [23]). We recall that the flow derivative of the optimal state process, valued in $\mathbb{R}^{d \times d}$, is solution to the SDE (see e.g. [27])

$$D_{X_t} X_s = I_d + \int_t^s D_x b^{a^*}(r, X_r) D_{X_t} X_r dr + D_x \sigma_j^{a^*}(r, X_r) D_{X_t} X_r dW_r^j, \quad t \leq s \leq T, \quad (3.5)$$

where we denote by $b^{a^*}(t, x) = b(x, a^*(t, x))$, $\sigma^{a^*}(t, x) = \sigma(x, a^*(t, x))$, and use the Einstein summation convention over the repeated index $j = 1, \dots, d$, with $\sigma_j^{a^*}$ (resp. σ_j) the j -th column of the matrix σ^{a^*} (resp. σ). Notice that $D_x b^{a^*} = D_x b + D_a b D_x a^*$, and $D_x \sigma_j^{a^*} = D_x \sigma_j + D_a \sigma_j D_x a^*$.

Remark 3.1. *We have an alternative representation (3.3) for the gradient of v , which avoids smoothness assumptions on the coefficients. It is expressed with \hat{Z}_T^t given by (see [21]):*

$$\hat{Z}_T^t = g(\hat{X}_T) \hat{H}_T^t + \int_t^T f(\hat{X}_s, \hat{a}(s, \hat{X}_s)) \hat{H}_s^t ds, \quad t \in [0, T], \quad (3.6)$$

with the so-called Malliavin weights \hat{H}_s^t , $t \leq s$, given by

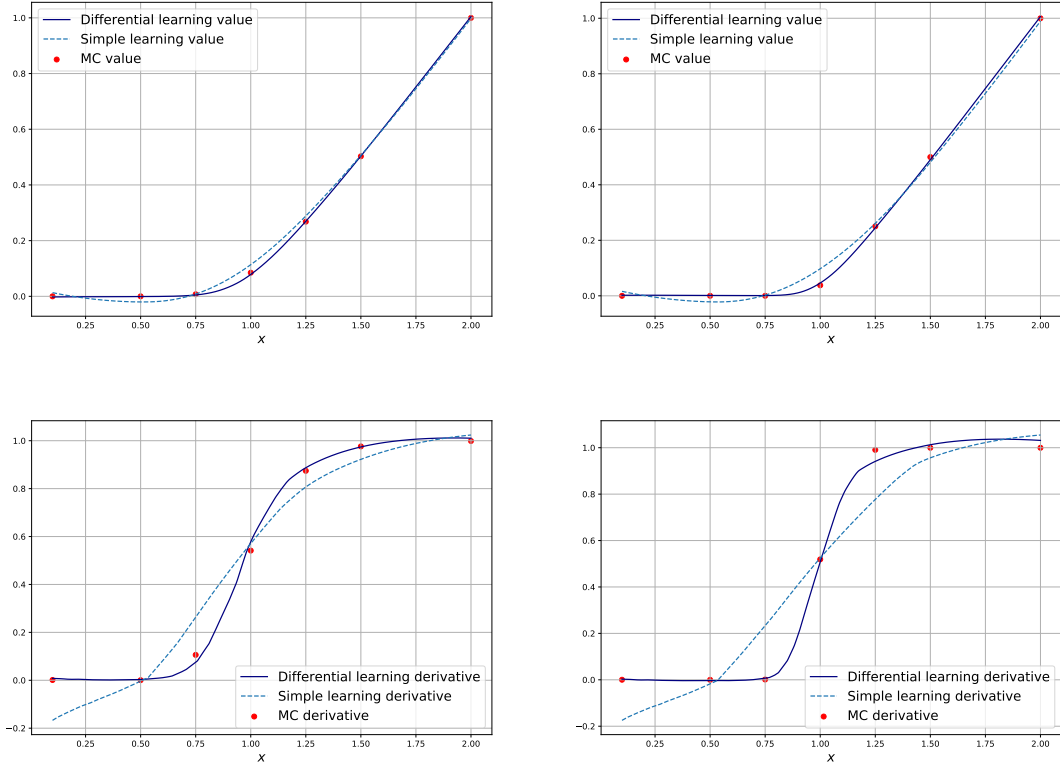
$$H_s^t = \frac{1}{s-t} \int_t^s \sigma^{-1}(t, \hat{X}_t)^\top \sigma^{-1}(r, \hat{X}_r) D_{\hat{X}_t} \hat{X}_r \sigma(t, \hat{X}_t) dW_r,$$

where $\sigma^{-1} = \sigma^\top (\sigma \sigma^\top)^{-1}$ is the right-inverse of the matrix σ assumed to be of full rank. Therefore, in the loss function L_{der}^* , instead of $Z_T^{*,t}$ as in (3.4), we can use alternately $Z_T^{*,t}$ as in (3.6), with \hat{X} approximated by X^* , and \hat{a} approximated by a^* .

To illustrate the interest of learning the derivative of the value function, we plot in Figure 1 the results obtained by learning the value and the derivative (*Differential regression learning*) or by learning just the value (*Simple learning*) of the call option price with market impact (see the application presented in Section 5.6).

As a reference, we compute the option price on chosen points $(t, x) \in \mathbb{R}_+ \times \mathbb{R}$ by Monte-Carlo, as explained in section 5.4.

In the differential regression learning method, we use a combination of the loss L_{val}^* and L_{der}^* in the training of the neural networks for approximating the value function and its derivative. We train alternately the value and the derivative of the network by taking a gradient step to minimize L_{val}^* every even number of epochs and a gradient step to minimize L_{der}^* every odd number of epochs. An alternative method would be to minimize a convex combination of L_{val}^* and L_{der}^* with weights w_{val} and $w_{der} = 1 - w_{val}$. These weights could be chosen by performing a grid search or a random search, such as advocated in [4] for the choice of neural network hyperparameters. Some theoretical arguments could also be



(a) $t = 0.5$

(b) $t = 0.9$

Figure 1: Value function values (first line) and derivatives (second line) obtained by *Differential Learning* (navy curve) (Algorithm 2), *Simple learning* (blue dashed curve) and Monte Carlo (red dots) plotted as functions of x , for fixed values of t .

derived in order to choose these weights, as it has been done in [33] to optimally choose the weights of the losses associated to different constraints of a PDE when using Physics Informed Neural Networks [28]. Our approach proves to be effective, as shown by the numerical results in Sections 5.5 and 5.6, and avoids the need to choose a value for this additional hyperparameter. The algorithmic implementation and the pseudo-codes are described in Section 5.2.

4 Pathwise learning

4.1 Pathwise martingale learning

This approach is based on the martingale representation related to relation (2.5), which leads by Itô's formula to the equation:

$$\hat{Y}_T^t = u(t, \hat{X}_t) + \int_t^T (D_x u(s, \hat{X}_s))^\top \sigma^{\hat{a}}(s, \hat{X}_s) dW_s, \quad t \in [0, T], \quad (4.1)$$

where we recall that \hat{Y}_T^t is given in (3.1), and denote $\sigma^{\hat{a}}(t, x) = \sigma(x, \hat{a}(t, x))$. This suggests to use a class of neural networks (NN) functions ϑ^η on $[0, T] \times \mathbb{R}^d$, with parameters η , for approximating the value function u , and a loss function

$$\begin{aligned} \hat{L}_{mar}(\eta) &= \mathbb{E} \left[\int_0^T |\hat{Y}_T^t - \vartheta^\eta(t, \hat{X}_t) - \int_t^T (D_x \vartheta^\eta(s, \hat{X}_s))^\top \sigma^{\hat{a}}(s, \hat{X}_s) dW_s|^2 dt \right] \\ &\simeq \mathbb{E} \left[\int_0^T |Y_T^{*,t} - \vartheta^\eta(t, X_t^*) - \int_t^T (D_x \vartheta^\eta(s, X_s^*))^\top \sigma^{a^*}(s, X_s^*) dW_s|^2 dt \right] \\ &=: L_{mar}^*(\eta). \end{aligned}$$

Alternately, we can use two classes of neural networks: one ϑ^η from $[0, T] \times \mathbb{R}^d$ into \mathbb{R} , with parameters η , for the approximation of u , and a second one \mathcal{Z}^δ from $[0, T] \times \mathbb{R}^d$ into \mathbb{R}^d , with parameters δ , for the approximation of $D_x u$. We then consider a loss function

$$\tilde{L}_{mar}^*(\eta, \delta) := \mathbb{E} \left[\int_0^T |Y_T^{*,t} - \vartheta^\eta(t, X_t^*) - \int_t^T \mathcal{Z}^\delta(s, X_s^*)^\top \sigma^{a^*}(s, X_s^*) dW_s|^2 dt \right].$$

Notice that compared to the deep BSDE approach in [13], which considers a loss function from the misfit between the l.h.s (the target) and r.h.s. of (4.1) at time 0, namely

$$\tilde{L}_{DBSDE}^*(y_0, \delta) := \mathbb{E} \left[|Y_T^{*,0} - y_0 - \int_0^T \mathcal{Z}^\delta(s, X_s^*)^\top \sigma^{a^*}(s, X_s^*) dW_s|^2 \right],$$

our loss functions L_{mar}^* or \tilde{L}_{mar}^* take into account the misfit between the l.h.s and r.h.s. of (4.1) at any time $t \in [0, T]$, since our goal is to approximate the solution u (and its derivative) on the whole domain $[0, T] \times \mathbb{R}^d$ (and not only at time $t = 0$).

4.2 Pathwise differential learning

We can further compute the pathwise derivative in the martingale representation relation (4.1) in order to obtain a second estimator linking the first and second derivatives of $u(t, x)$. Indeed, by [7], we have

$$\begin{aligned} D_{\hat{X}_t} \hat{Y}_T^t &= D_x u(t, \hat{X}_t) + \int_t^T \left([D_x \sigma^{\hat{a}}(s, \hat{X}_s) \bullet_3 D_{\hat{X}_t} \hat{X}_s] \bullet_1 D_x u(s, \hat{X}_s) \right. \\ &\quad \left. + \sigma^{\hat{a}}(s, \hat{X}_s)^\top D_x^2 u(s, \hat{X}_s) D_{\hat{X}_t} \hat{X}_s \right)^\top dW_s, \quad t \in [0, T]. \end{aligned}$$

This suggests to use a class of neural networks (NN) functions ϑ^η on $[0, T] \times \mathbb{R}^d$, with parameters η , for approximating the value function u , and a loss function

$$L_{dermar}^*(\eta) = \mathbb{E} \left[\int_0^T \left| Z_T^{*,t} - D_x \vartheta^\eta(t, X_t) - \int_t^T \left([D_x \sigma^{a^*}(s, X_s) \bullet_3 D_{X_t} X_s] \bullet_1 D_x \vartheta^\eta(s, X_s) + \sigma^{a^*}(s, X_s)^\top D_x^2 \vartheta^\eta(s, X_s) D_{X_t} X_s \right)^\top dW_s \right|^2 dt \right],$$

where we recall that $Z_T^{*,t}$ is given in (3.4), and we omit the superscript $*$ in the approximation of the optimal state process $X = X^*$. Alternatively, we can use three classes of neural networks: one ϑ^η from $[0, T] \times \mathbb{R}^d$ into \mathbb{R} , with parameters η , for the approximation of u , a second one \mathcal{Z}^δ from $[0, T] \times \mathbb{R}^d$ into \mathbb{R}^d , with parameters δ , for the approximation of $D_x u$, and a third one Γ^ϵ from $[0, T] \times \mathbb{R}^d$ into \mathbb{S}^d , with parameters ϵ , for the approximation of $D_{xx} u$, and consider a loss function

$$\tilde{L}_{dermar}^*(\delta, \epsilon) = \mathbb{E} \left[\int_0^T \left| Z_T^{*,t} - \mathcal{Z}^\delta(t, X_t) - \int_t^T \left([D_x \sigma^{a^*}(s, X_s) \bullet_3 D_{X_t} X_s] \bullet_1 \mathcal{Z}^\delta(s, X_s) + \sigma^{a^*}(s, X_s)^\top \Gamma^\epsilon(s, X_s) D_{X_t} X_s \right)^\top dW_s \right|^2 dt \right].$$

As with the Differential regression learning method presented in Section 3, the neural network can be trained either by minimising a convex combination of the losses L_{mar}^* and L_{dermar}^* or by minimising these losses individually. During our numerical experiment, we minimised these two losses individually, but contrary to the algorithm used in the Differential regression learning, for each epoch, a gradient step was made to minimise L_{mar}^* and then another one was made to minimize L_{dermar}^* .

Remark 4.1. *This optimisation scheme was found to be more effective when optimising the neural network parameters for the Pathwise differential learning. For the Differential regression learning method, making a gradient step on only one of these two losses at each epoch gave better results. The difference between these two optimization schemes lies in the fact that if both the losses L_{mar}^* and L_{dermar}^* are optimised during an epoch, these two losses are computed using the "old" network weights η , then these weights are modified two times, first by making a gradient step to minimize L_{mar}^* , and then by taking another gradient step to minimize L_{dermar}^* , as written below*

One epoch:

$$\begin{aligned} \eta' &\leftarrow \eta - \nabla_\eta L_{mar}^*(\eta), \\ \eta'' &\leftarrow \eta' - \nabla_\eta L_{dermar}^*(\eta). \end{aligned}$$

When the network is optimised by minimizing alternatively one of these two losses at each epoch, as in the Differential regression method, one of the losses, say L_{mar}^* , is computed

using the "old" weights η . A gradient step is then made to minimize this loss and obtain new network weights η' , which are then used in the next epoch to compute the loss L_{mar}^* and make the next gradient step, as written below

One epoch:

$$\eta' \leftarrow \eta - \nabla_{\eta} L_{mar}^*(\eta),$$

Next epoch:

$$\eta'' \leftarrow \eta' - \nabla_{\eta} L_{dermar}^*(\eta').$$

5 Numerical results

In this section, we detail the implementation of the methods presented above. Our algorithms are discretised in time for the training of the processes and for the integrals that appear in the loss functions, and which are approximated by Riemann sums. In the sequel, we are then given a mesh grid $\mathcal{T}_N = \{0 = t_0 < t_1 < \dots < t_N = T\}$ of $[0, T]$ with $\Delta t_n = t_{n+1} - t_n$, for $n = 0, \dots, N - 1$.

Our codes are written in Python and we use the Tensorflow library to implement the neural networks and compute the derivatives present in our calculations by auto-differentiation (AAD).

Finally, we illustrate our results with some examples of applications in finance.

5.1 Approximation of the optimal control

As a first step, we consider a neural network a_{θ} from $[0, T] \times \mathbb{R}^d$ into $A \subset \mathbb{R}^q$ for the approximation of the feedback control, and the associated discretised state process

$$X_{t_{n+1}}^{\theta} = X_{t_n}^{\theta} + b(X_{t_n}^{\theta}, a_{\theta}(t_n, X_{t_n}^{\theta}))\Delta t + \sigma(X_{t_n}^{\theta}, a_{\theta}(t_n, X_{t_n}^{\theta}))\Delta W_{t_n}, \quad n = 0, \dots, N - 1,$$

starting from $X_0 \sim \mu_0$ (probability distribution on \mathbb{R}^d), and where $\Delta W_{t_n} = W_{t_{n+1}} - W_{t_n}$. As in [15], to constrain the output of the neural network a_{θ} to be in the control space A , we define a custom activation function σ_A for the output layer of the network. This activation function σ_A is chosen depending on the form of the control space A . When $A = \mathbb{R}^q$, σ_A is equal to the identity function. When the control space is of the form $A = \prod_{i=1}^q [a_i, \infty)$, one can take the component-wise ReLU activation function (possibly shifted and scaled); when $A = \prod_{i=1}^q [a_i, b_i]$, for $a_i \leq b_i$, $i = 1, \dots, q$, one can take the component-wise sigmoid activation function (possibly shifted and scaled). For the numerical experiments presented here, we used the ELU (Exponential Linear Unit) activation function, defined as

$$ELU(x) = \begin{cases} x & x > 0 \\ \alpha(e^x - 1) & x \leq 0, \end{cases}$$

with parameter α for the hidden layers.

The structure of the neural networks used to approximate the feedback control is represented in Figure 2. It is composed of two dense feed-forward sub-networks composed of two layers of n neurons, taking respectively the time t and the state x as input. The outputs of these two sub-network, which are in \mathbb{R}^n , are then concatenated and inputed in a third dense network composed of two layers of n neurons and a last layer of q neurons which outputs the approximation of the control in \mathbb{R}^q . This structure adds more flexibility compared to the network structure usually implemented, where the time and state variables are directly concatenated and passed through a dense feed-forward network. It allows to use different activation functions in each sub-network and adapts well to situations where the network is used to approximate a function which has very different behaviors in its time and state variables. The same structure is used for the neural networks used to approximate the value function by Differential Regression learning or Pathwise learning. In the applications presented in this article, we used neural networks with $n = 50$ neurons per layer and $q = 1$.

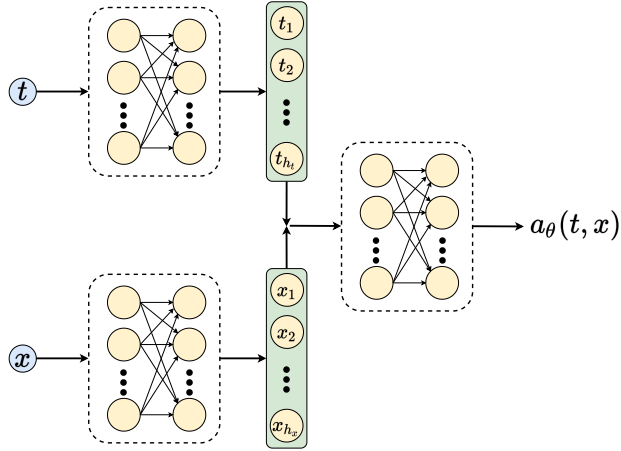


Figure 2: Structure of the neural network used to approximate the optimal control and value function.

For the training of the neural network control a_θ , we use a batch of M independent trajectories $\{x_{t_n}^{m,\theta}, t_n \in \mathcal{T}_N\}$, $m = 1, \dots, M$, of $\{X_{t_n}^\theta, t_n \in \mathcal{T}_N\}$, and apply a stochastic gradient ascent method to the empirical gain function:

$$J_M(\theta) = \frac{1}{M} \sum_{m=1}^M \left[g(x_T^{m,\theta}) + \sum_{n=0}^{N-1} f(x_{t_n}^{m,\theta}, a_\theta(t_n, x_{t_n}^{m,\theta})) \Delta t_n \right].$$

The pseudo-code is described in Algorithm 1. The output of this algorithm yields a parameter θ^* , and so an approximation of the optimal feedback control with $a^* = a_{\theta^*}$, and of the associated optimal state process with $X^* = X^{\theta^*}$. In the sequel, to alleviate notations, we shall omit the superscript $*$, and simply denote a and X .

Algorithm 1: Deep learning scheme to solve the stochastic control problem (2.3)

Result: A set of optimized parameters θ^* ;
Initialize the learning rate l and the neural network a_θ ;
Generate an \mathbb{R}^{N+1} -valued time grid $0 = t_0 < t_1 < \dots < t_N = T$ with time steps $(\Delta t_n)_{n=0, \dots, N-1}$;
Generate a batch of M starting points $X_0 \sim \mu_0$ and Brownian increments $(\Delta W_{t_n})_{n=0, \dots, N-1}$ in \mathbb{R}^d ;
for each batch element m **do**
 Compute the trajectory $(x_{t_n}^{m, \theta})_{n=0, \dots, N}$ through the scheme

$$x_{t_{n+1}}^{m, \theta} = x_{t_n}^{m, \theta} + b(x_{t_n}^{m, \theta}, a_\theta(t_n, x_{t_n}^{m, \theta}))\Delta t_n + \sigma(x_{t_n}^{m, \theta}, a_\theta(t_n, x_{t_n}^{m, \theta}))\Delta w_{t_n}^m,$$

 from the generated starting point $x_{t_0}^m$ and Brownian increments $(\Delta w_{t_n}^m)_{n=0, \dots, N-1}$;
end
for each epoch **do**
 Compute the batch loss

$$J_M(\theta) = \frac{1}{M} \sum_{m=1}^M \left[g(x_T^{m, \theta}) + \sum_{n=0}^{N-1} f(x_{t_n}^{m, \theta}, a_\theta(t_n, x_{t_n}^{m, \theta}))\Delta t_n \right]$$

 Compute the gradients $\nabla_\theta J_M(\theta)$;
 Update $\theta \leftarrow \theta - l \nabla_\theta J_M(\theta)$;
end
Return: The set of optimized parameters θ^* ;

5.2 Differential regression learning algorithm

We consider a neural network ϑ^η from $[0, T] \times \mathbb{R}^d$ into \mathbb{R} for the approximation of the value function. The derivatives $D_x g$, $D_x f$, $D_x b$, $D_x \sigma$, $D_x a$, and $D_x \vartheta^\eta$ that appear in the differential regression learning methods are computed straightforwardly by auto-differentiation. Concerning the flow derivative of the approximate optimal state process, it is computed by time discretization of (3.5), which can be efficiently obtained by storing the one-step derivatives:

$$D_{X_{t_n}} X_{t_{n+1}} = I_d + D_x b^{a^*}(t_n, X_{t_n})\Delta t_n + \sum_{j=1}^d D_x \sigma_j^{a^*}(t_n, X_{t_n})\Delta W_{t_n}^j, \quad n = 0, \dots, N-1,$$

and then use the chain rule

$$D_{X_{t_n}} X_{t_p} = D_{X_{t_n}} X_{t_{n+1}} \cdots D_{X_{t_{p-1}}} X_{t_p}, \quad \text{for } n < p \in \llbracket 0, N \rrbracket$$

The target payoff and its derivative are then computed as

$$Y_T^{t_n} = g(X_T) + \sum_{p=n}^{N-1} f^{a^*}(t_p, X_{t_p})\Delta t_p, \quad n = 0, \dots, N,$$

$$Z_T^{t_n} = (D_{X_{t_n}} X_T)^\top D_x g(X_T) + \sum_{p=n}^{N-1} (D_{X_{t_n}} X_{t_p})^\top D_x f^{a^*}(t_p, X_{t_p})\Delta t_p,$$

with the convention that the above sum over p is zero when $n = N$.

For the training of the neural network ϑ^η , we use a batch of M independent samples $(x_{t_n}^m, y_T^{m,t_n}, z_T^{m,t_n})$, $m = 1, \dots, M$, of $(X_{t_n}, Y_T^{t_n}, Z_T^{t_n})$, $n = 0, \dots, N$, and apply stochastic gradient descent for the minimization of the mean squared error functions

$$\begin{aligned} MSE_{val}(\eta) &= \frac{1}{M} \sum_{m=1}^M \sum_{n=0}^{N-1} |y_T^{m,t_n} - \vartheta^\eta(t_n, x_{t_n}^m)|^2 \Delta t_n \\ MSE_{der}(\eta) &= \frac{1}{M} \sum_{m=1}^M \sum_{n=0}^{N-1} \frac{1}{\|z_T^{t_n}\|^2} |z_T^{m,t_n} - D_x \vartheta^\eta(t_n, x_{t_n}^m)|^2 \Delta t_n. \end{aligned}$$

Here, as in [14] (Appendix 2), we normalize the derivative loss by the L_2 norm of the target derivative computed along the batch dimension $\|z_T^{t_n}\|^2 := (\sum_{m=1}^M \sqrt{z_T^{t_n}})^2$.

The pseudo-code is described in Algorithm 2.

Remark 5.1. Notice that in the above expressions of the mean squared errors, the neural network is trained from the time $t_0 = 0$ up to time $t_{N-1} < T$ and is thus not trained on the terminal condition of the PDE (2.1). This choice is justified by the fact that the neural network is already implicitly trained to fit the terminal condition at time T since the terminal function g appears in the losses. Furthermore, we observed that the regularity of the terminal function affects the performance of the neural network. If the terminal function is at least of class C^1 , no problem arises as the regularity of the solution to the PDE (2.1) is the same on the domain $[0, T) \times \mathbb{R}^d$ and on the terminal domain $\{T\} \times \mathbb{R}^d$. If we use a neural network ϑ^η of regularity C^1 , we will then be able to approximate the PDE solution on the entire domain $[0, T] \times \mathbb{R}^d$. However, if the terminal condition's regularity is less than C^1 , it will be difficult for the neural network to approximate the PDE solution on the entire domain $[0, T] \times \mathbb{R}^d$. Indeed, the solution of parabolic PDEs is often smoother than its terminal (or initial) condition, thus the neural network will have to approximate a function that has a continuous first derivative on the domain $[0, T) \times \mathbb{R}^d$ and a discontinuous first derivative on $\{T\} \times \mathbb{R}^d$. If the neural network used is not C^1 , which is the case for a network with ReLU activation functions for example, the network will give a good approximation of the terminal condition but will give a worst fit of the solution on the domain $[0, T) \times \mathbb{R}^d$, and particularly of its derivatives. On the contrary, if the neural network used is C^1 , which is the case when the ELU activation function is used, the network will give a good approximation of the solution on $[0, T) \times \mathbb{R}^d$ but will give a worse approximation of the terminal condition. The difficulty thus comes from the fact that we try to obtain a solution on the entire domain of the PDE. As the terminal condition is known and the quantity of interest is the solution of the PDE (2.1) on the domain $[0, T) \times \mathbb{R}^d$, we choose to use a C^1 neural network trained on this domain.

Algorithm 2: Deep learning scheme for Differential Regression learning

Result: A set of optimized parameters η^* ;
 Initialize the learning rate l , the neural networks ϑ^η ;
 Generate an \mathbb{R}^{N+1} -valued time grid $0 = t_0 < t_1 < \dots < t_N = T$ with time steps $(\Delta t_n)_{n=0, \dots, N-1}$;
 Generate a batch of M starting points $X_0 \sim \mu_0$ and Brownian increments $(\Delta W_{t_n})_{n=0, \dots, N}$ in \mathbb{R}^d ;
for each batch element m **do**
 Compute the trajectory $(x_{t_n}^m)_{n=0, \dots, N}$ through the scheme

$$x_{t_{n+1}}^m = x_{t_n}^m + \mathbf{b}^{a^*}(t_n, x_{t_n}^m) \Delta t_n + \sigma^{a^*}(t_n, x_{t_n}^m) \Delta w_{t_n}^m,$$

 from the generated starting point $x_{t_0}^m$, Brownian increments $(\Delta w_{t_n}^m)_{n=0, \dots, N-1}$ and previously trained control $a = a_{\theta^*}$;
 Compute the value and derivative targets $(y_T^{m, t_n})_{n=0, \dots, N}$ and $(z_T^{m, t_n})_{n=0, \dots, N}$;
end
for each epoch **do**
 if Epoch number is even **then**
 Compute, for every batch element m , the integral $\sum_{n=0}^{N-1} |y_T^{m, t_n} - \vartheta^\eta(t_n, x_{t_n}^m)|^2 \Delta t_n$;
 Compute the batch loss $MSE_{val}(\eta)$;
 Compute the gradient $\nabla_\eta MSE_{val}(\eta)$;
 Update $\eta \leftarrow \eta - l \nabla_\eta MSE_{val}(\eta)$;
 end
 else
 Compute, for every batch element m , the integral $\sum_{n=0}^{N-1} |z_T^{m, t_n} - D_x \vartheta^\eta(t_n, x_{t_n}^m)|^2 \Delta t_n$;
 Compute the batch loss $MSE_{der}(\eta)$;
 Compute the gradient $\nabla_\eta MSE_{der}(\eta)$;
 Update $\eta \leftarrow \eta - l \nabla_\eta MSE_{der}(\eta)$;
 end
end
Return: The set of optimized parameters η^* ;

5.3 Pathwise learning algorithms

We consider a neural network ϑ^η from $[0, T] \times \mathbb{R}^d$ into \mathbb{R} for the approximation of the value function. For the training of this neural network, we use a batch of M independent samples $(x_{t_n}^m, y_T^{m, t_n}, \Delta w_{t_n}^m)$, $m = 1, \dots, M$, of $(X_{t_n}, Y_T^{t_n}, \Delta W_{t_n})$, $n = 0, \dots, N$, and apply stochastic gradient descent for the minimization of the mean squared error function

$$\begin{aligned}
 MSE_{mar}(\eta) = & \frac{1}{M} \sum_{m=1}^M \sum_{n=0}^{N-1} \left| y_T^{m, t_n} - \vartheta^\eta(t_n, x_{t_n}^m) \right. \\
 & \left. - \sum_{p=n}^{N-1} (D_x \vartheta^\eta(t_p, x_{t_p}^m))^\top \sigma(x_{t_p}^m, \mathbf{a}^*(t_p, x_{t_p}^m)) \Delta w_{t_p}^m \right|^2 \Delta t_n,
 \end{aligned} \tag{5.1}$$

The pseudo-code for the pathwise martingale learning is described in Algorithm 3.

Algorithm 3: Deep learning scheme for Pathwise martingale learning with 1 NN

Result: A set of optimized parameters η^* ;
 Initialize the learning rate l , the neural networks ϑ^η ;
 Generate an \mathbb{R}^{N+1} -valued time grid $0 = t_0 < t_1 < \dots < t_N = T$ with time steps $(\Delta t_n)_{n=0, \dots, N-1}$;
 Generate a batch of M starting points $X_0 \sim \mu_0$ and Brownian increments $(\Delta W_{t_n})_{n=0, \dots, N}$ in \mathbb{R}^d ;
for each batch element m do
 Compute the trajectory $(x_{t_n}^m)_{n=0, \dots, N}$ through the scheme

$$x_{t_{n+1}}^m = x_{t_n}^m + b^{a^*}(t_n, x_{t_n}^m) \Delta t_n + \sigma^{a^*}(t_n, x_{t_n}^m) \Delta w_{t_n}^m,$$

 from the generated starting point $x_{t_0}^m$, Brownian increments $(\Delta w_{t_n}^m)_{n=0, \dots, N-1}$ and previously trained control $a = a_{\theta^*}$;
 Compute the value target $(y_T^{m, t_n})_{n=0, \dots, N}$;
end
for each epoch do
 Compute, for every batch element m , the integral

$$\sum_{n=0}^{N-1} \left| y_T^{m, t_n} - \vartheta^\eta(t_n, x_{t_n}^m) - \sum_{p=n}^{N-1} (D_x \vartheta^\eta(t_p, x_{t_p}^m))^\top \sigma^{a^*}(t_p, x_{t_p}^m) \Delta w_{t_p}^m \right|^2 \Delta t_n;$$

 Compute the batch loss $MSE_{mar}(\eta)$;
 Compute the gradient $\nabla_\eta MSE_{mar}(\eta)$;
 Update $\eta \leftarrow \eta - l \nabla_\eta MSE_{mar}(\eta)$;
end
Return: The set of optimized parameters η^* ;

Alternately, we can use another neural network \mathcal{Z}^δ from $[0, T] \times \mathbb{R}^d$ into \mathbb{R}^d for the approximation of the gradient of the solution, and then use the mean squared error function

$$\begin{aligned} \tilde{MSE}_{mar}(\eta, \delta) = \frac{1}{M} \sum_{m=1}^M \sum_{n=0}^{N-1} & \left| y_T^{m, t_n} - \vartheta^\eta(t_n, x_{t_n}^m) \right. \\ & \left. - \sum_{p=n}^{N-1} (\mathcal{Z}^\delta(t_p, x_{t_p}^m))^\top \sigma^{a^*}(x_{t_p}^m) \Delta w_{t_p}^m \right|^2 \Delta t_n. \end{aligned}$$

The pseudo-code for the pathwise martingale learning with two neural networks is described in Algorithm 7 in Appendix A.

For the differential version of this algorithm, we also use a neural network ϑ^η from $[0, T] \times \mathbb{R}^d$ into \mathbb{R} for the approximation of the value function that we train by using the same batch of M independent samples and applying stochastic gradient descent for the minimization of both the mean squared error functions defined in (5.1) and the following one:

$$\begin{aligned}
MSE_{dermar}(\eta) = & \frac{1}{M} \sum_{m=1}^M \sum_{n=0}^{N-1} \left| z_T^{m,t_n} - D_x \vartheta^\eta(t_n, x_{t_n}^m) \right. \\
& - \sum_{p=n}^{N-1} \left([D_x \sigma^{a^*}(t_p, x_{t_p}^m) \bullet_3 D_{x_{t_n}} x_{t_p}^m] \bullet_1 D_x \vartheta^\eta(t_p, x_{t_p}^m) \right. \\
& \left. \left. + \sigma^{a^*}(t_p, x_{t_p}^m)^\top D_{xx} \vartheta^\eta(t_p, x_{t_p}^m) D_{x_{t_n}} x_{t_p}^m \right)^\top \Delta w_{t_p}^m \right|^2 \Delta t_n.
\end{aligned}$$

The pseudo-code is described in Algorithm 4.

Algorithm 4: Deep learning scheme for Pathwise differential learning with 1 NN

Result: A set of optimized parameters η^* ;

Initialize the learning rate l , the neural networks ϑ^η ;

Generate an \mathbb{R}^{N+1} -valued time grid $0 = t_0 < t_1 < \dots < t_N = T$ with time steps $(\Delta t_n)_{n=0, \dots, N-1}$;

Generate a batch of M starting points $X_0 \sim \mu_0$ and Brownian increments $(\Delta W_{t_n})_{n=0, \dots, N}$ in \mathbb{R}^d ;

for each batch element m do

 Compute the trajectory $(x_{t_n}^m)_{n=0, \dots, N}$ through the scheme

$$x_{t_{n+1}}^m = x_{t_n}^m + b^{a^*}(t_n, x_{t_n}^m) \Delta t_n + \sigma^{a^*}(t_n, x_{t_n}^m) \Delta w_{t_n}^m,$$

 from the generated starting point $x_{t_0}^m$, Brownian increments $(\Delta w_{t_n}^m)_{n=0, \dots, N-1}$ and previously trained control $a = a_{\theta^*}$;

 Compute the value and derivative targets $(y_T^{m,t_n})_{n=0, \dots, N}$ and $(z_T^{m,t_n})_{n=0, \dots, N}$;

end

for each epoch do

 Compute, for every batch element m , the integral

$$\sum_{n=0}^{N-1} \left| y_T^{m,t_n} - \vartheta^\eta(t_n, x_{t_n}^m) - \sum_{p=n}^{N-1} (D_x \vartheta^\eta(t_p, x_{t_p}^m))^\top \sigma^{a^*}(t_p, x_{t_p}^m) \Delta w_{t_p}^m \right|^2 \Delta t_n;$$

 Compute the batch loss $MSE_{mar}(\eta)$;

 Compute the gradient $\nabla_\eta MSE_{mar}(\eta)$;

 Update $\eta \leftarrow \eta - l \nabla_\eta MSE_{mar}(\eta)$;

 Compute, for every batch element m , the integral

$$\sum_{n=0}^{N-1} \left| z_T^{m,t_n} - D_x \vartheta^\eta(t_n, x_{t_n}^m) - \sum_{p=n}^{N-1} \left([D_x \sigma^{a^*}(t_p, x_{t_p}^m) \bullet_3 D_{x_{t_n}} x_{t_p}^m] \bullet_1 D_x \vartheta^\eta(t_p, x_{t_p}^m) \right. \right. \\ \left. \left. + \sigma^{a^*}(t_p, x_{t_p}^m)^\top D_{xx} \vartheta^\eta(t_p, x_{t_p}^m) D_{x_{t_n}} x_{t_p}^m \right)^\top \Delta w_{t_p}^m \right|^2 \Delta t_n;$$

 Compute the batch loss $MSE_{dermar}(\eta)$;

 Compute the gradient $\nabla_\eta MSE_{dermar}(\eta)$;

 Update $\eta \leftarrow \eta - l \nabla_\eta MSE_{dermar}(\eta)$;

end

Return: The set of optimized parameters η^* ;

Alternately, in addition to the NN ϑ^η for u , we can use neural networks \mathcal{Z}^δ and Γ^ϵ for

the gradient and the Hessian that we train with the loss function

$$\begin{aligned} \tilde{MSE}_{dermar}(\delta, \epsilon) = & \frac{1}{M} \sum_{m=1}^M \sum_{n=0}^{N-1} \left| z_T^{m,t_n} - \mathcal{Z}^\delta(t_n, x_{t_n}^m) \right. \\ & - \sum_{p=n}^{N-1} \left([D_x \sigma^{a^*}(t_p, x_{t_p}^m) \bullet_3 D_{x_{t_n} x_{t_p}^m}] \bullet_1 \mathcal{Z}^\delta(t_p, x_{t_p}^m) \right. \\ & \left. \left. + \sigma^{a^*}(t_p, x_{t_p}^m)^\top \Gamma^\epsilon(t_p, x_{t_p}^m) D_{x_{t_n} x_{t_p}^m} \right)^\top \Delta w_{t_p}^m \right|^2 \Delta t_n, \end{aligned}$$

where $D_{x_{t_n} x_{t_p}^m}$ denotes the flow derivative of the approximate optimal state process at time t_p w.r.t the state at time t_n along the path m of the batch.

The pseudo-code for this version using three neural networks is described in Algorithm 8 in Appendix A.

5.4 Validation tests

The deep learning methods described above provide an approximation ϑ of the solution u to the PDE, which relies up-front on the approximation a^θ of the optimal control \hat{a} arising from the dual stochastic control representation.

We can test and validate the convergence and accuracies of these approximations as follows. On the one hand, as in the DGM and PINN methods, see [30] and [28], we can compute the losses \mathcal{L}_{res} and \mathcal{L}_{term} , associated respectively to the residual and to the terminal condition of the partial differential equation (2.1)

$$\begin{aligned} \mathcal{L}_{res} &:= \frac{1}{|\mathcal{T}||\chi|} \sum_{t \in \mathcal{T}, x \in \chi} \left| \partial_t \vartheta^\eta + H(x, D_x \vartheta^\eta, D_x^2 \vartheta^\eta) \right|^2, \\ \mathcal{L}_{term} &:= \frac{1}{|\chi|} \sum_{x \in \chi} \left| \vartheta^\eta(T, x) - g(x) \right|^2, \end{aligned} \tag{5.2}$$

where the time grid \mathcal{T} is composed of times that were not used during the network training, so as to verify the generalisation of the solution obtained, and χ is a bounded space grid in \mathbb{R}^d . As the state diffusion $(X_t^\theta)_{0 \leq t \leq T}$ is not bounded, the bounds of the space grid are fixed arbitrarily depending on the domain of interest. Alternatively, these bounds could be chosen based on the distribution of the values attained during the computation of the diffusion scheme of $(X_t^\theta)_{0 \leq t \leq T}$.

On the other hand, by noting that the optimal control should satisfy the optimality condition

$$D_a b(x, \hat{a}) \cdot D_x u(t, x) + \frac{1}{2} \text{Tr}_{1,2}(D_a \sigma \sigma^\top(x, \hat{a}) \bullet_2 D_{xx} u(t, x)) + D_a f(x, \hat{a}) = 0,$$

we can check the accuracy the approximation \mathbf{a}_θ of the optimal control by computing the following loss

$$\begin{aligned} \mathcal{L}_{optim} = \frac{1}{|\mathcal{T}||\mathcal{X}|} \sum_{t \in \mathcal{T}, x \in \mathcal{X}} & \left| D_a \mathbf{b}(x, \mathbf{a}_\theta) D_x \vartheta^\eta(t, x) + \frac{1}{2} \text{Tr}_{1,2}(D_a \sigma \sigma^\top(x, \mathbf{a}_\theta)) \bullet_2 D_{xx} \vartheta^\eta(t, x) \right. \\ & \left. + D_a f(x, \mathbf{a}_\theta) \right|^2, \end{aligned}$$

on the same grid $\mathcal{T} \times \mathcal{X}$ as before.

Another validation method, which is more graphical, consists in approximating numerically the optimal control as described in Section 5.1 and then computing the value function and its first derivative for some chosen points (t, x) by Monte Carlo simulations:

$$\begin{aligned} \vartheta_{MC}(t, x) &= \frac{1}{M} \sum_{m=1}^M \left[g(x_{t_N}^{m,t,x}) + \sum_{p=n}^{N-1} f(x_{t_p}^{m,t,x}, \mathbf{a}_\theta(t_p, x_{t_p}^{m,t,x})) \Delta t_p \right], \\ D_x \vartheta_{MC}(t, x) &= \frac{1}{M} \sum_{m=1}^M \left[(D_x x_{t_N}^{m,t,x})^\top D_x g(x_{t_N}^{m,t,x}) \right. \\ & \quad + \sum_{p=n}^{N-1} \left((D_x x_{t_p}^{m,t,x})^\top D_x f(x_{t_p}^{m,t,x}, \mathbf{a}_\theta(t_p, x_{t_p}^{m,t,x})) \right. \\ & \quad \left. \left. + (D_x \mathbf{a}_\theta(t_p, x_{t_p}^{m,t,x}) D_x x_{t_p}^{m,t,x})^\top D_a f(x_{t_p}^{m,t,x}, \mathbf{a}_\theta(t_p, x_{t_p}^{m,t,x})) \right) \Delta t_p \right], \end{aligned}$$

with $t = t_n$. We then plot these Monte Carlo points alongside the value functions obtained by using neural networks to check that the machine learning methods described in the previous sections are able to approximate the value function corresponding to the approximated optimal control \mathbf{a}_θ .

5.5 Example of Merton portfolio selection

We consider the Bellman equation:

$$\begin{cases} \partial_t u + \sup_{a \in \mathbb{R}} \left[a x b D_x u + \frac{1}{2} a^2 x^2 \sigma^2 D_x^2 u \right] = 0, & (t, x) \in [0, T) \times (0, \infty), \\ u(T, x) = g(x), & x \in (0, \infty), \end{cases}$$

which arises from the Merton portfolio selection problem where an agent invests a proportion $\alpha = (\alpha_t)_t$ of her wealth $X = X^\alpha$ in a stock following a Black-Scholes model with rate of return $b \in \mathbb{R}$, and constant volatility $\sigma > 0$. The controlled wealth dynamics is then governed by

$$dX_t = X_t \alpha_t b dt + X_t \alpha_t \sigma dW_t,$$

and the goal of the investor is to maximize over α her expected terminal wealth $\mathbb{E}[g(X_T)]$, with g some utility function, i.e. concave and nondecreasing, on $(0, \infty)$.

When the utility function g is of power type, i.e. $g(x) = x^\gamma/\gamma$, for some $\gamma < 1$, $\gamma \neq 0$, it is well-known that the optimal control is constant equal to

$$\hat{\alpha} = \frac{b}{\sigma^2(1-\gamma)},$$

while the value function is explicitly given by

$$u(t, x) = e^{\rho(T-t)}g(x), \quad \text{with} \quad \rho = \frac{b^2}{2\sigma^2} \frac{\gamma}{1-\gamma}.$$

These closed-form expressions serve as benchmarks for comparing our results computed by the differential learning algorithms.

In order to check that the value function approximation obtained is a lower bound of the true one, we compute in Table 1 the difference between the closed form value function and the estimation of the value function on points (t, x) obtained by computing the expectation (2.5) by Monte Carlo on $1e^6$ trajectories controlled by the Deep Learning approximation of the optimal control. We compute the value functions on a grid $t \in \{0, 0.5, 0.9\}$, $x \in \{1e^{-2}, 0.5, 0.75, 1, 1.25, 1.5, 2\}$ with parameters $b = 0.2$, $\sigma = 0.2$ and power utility with exponent $\gamma = 0.5$ and present in the table the difference between the closed form value and the Monte Carlo approximation. For clarity of presentation we present the results averaged over t in this table.

	$x = 1e^{-2}$	$x = 0.5$	$x = 0.75$	$x = 1$	$x = 1.25$	$x = 1.5$	$x = 2$
Difference closed - MC	$2.699e^{-4}$	$1.811e^{-3}$	$2.208e^{-3}$	$2.543e^{-3}$	$2.839e^{-3}$	$3.106e^{-3}$	$3.582e^{-3}$

Table 1: Difference between the closed form value function and the value computed by Monte Carlo on $1e^6$ trajectories on points $x \in \{1e^{-2}, 0.5, 0.75, 1, 1.25, 1.5, 2\}$ and averaged over times $t \in \{0, 0.5, 0.9\}$ for the Merton problem with parameters $b = 0.2$, $\sigma = 0.2$ and power utility with exponent $\gamma = 0.5$.

We compute in Table 2, the residual losses defined in (5.2) for the NN ϑ^η obtained by the various deep learning methods: the differential learning scheme (Algorithm 2), the pathwise martingale learning with 1 NN (Algorithm 3) and the pathwise differential learning with 1 NN (Algorithm 4). Since two gradient steps are performed during each training epoch of the Pathwise differential learning method, we indicate the training time for 500 epochs for this method whereas the training time of the two other methods is indicated for 1000 epochs. For each of these algorithms, 8192 starting points and Brownian trajectories are used in order to train the neural networks. We also provide the training time for each of these algorithms. On this table we see that the Pathwise differential learning method is

the slowest to train but yields the best results in terms of residual and terminal losses. We see that for all three methods the difference between the residual loss only and the sum of residual and terminal loss is small, meaning that with all three methods the neural network managed to fit the terminal condition of the PDE during the training.

	Diff. regr. learning	Path. 1NN	Path. diff. 1NN
Residual loss	$1.538e^{-1}$	$1.752e^{-1}$	$7.872e^{-2}$
Residual loss + terminal loss	$1.548e^{-1}$	$1.758e^{-1}$	$7.894e^{-2}$
Training time	274s 1000 epochs	297s 1000 epochs	525s 500 epochs

Table 2: Residual and boundary losses computed on a 102x102 time and space grid with $t \in [0, 0.9]$ and $x \in [1e^{-2}, 2]$ for the Merton problem with parameters $b = 0.2$, $\sigma = 0.2$ and power utility with exponent $\gamma = 0.5$.

We plot the value function $\vartheta^\eta(t, x)$ and its derivatives $\partial_x \vartheta^\eta(t, x)$ and $\partial_{xx} \vartheta^\eta(t, x)$ for fixed values $t = 0$, $t = 0.5$, $t = 0.9$, and for parameter values $b = 0.2$, $\sigma = 0.2$, $\gamma = 0.5$, and compare it with the closed-form solution of the problem. Figure 3 corresponds to the Differential regression learning method, Figure 4 corresponds to the pathwise martingale learning while Figure 5 corresponds to the pathwise differential learning method. These graphs are coherent with the results presented in Table 2. We see that the Pathwise differential provides the best fit, in particular for the first and second derivatives of the solution, followed by the Differential regression method. The Pathwise method provides a good fit for the value of the PDE solution but does not manage to fit very well its first and second derivatives for small values of x .

5.6 Example of the Black-Scholes model with linear market impact

We consider the option pricing problem with linear market impact as studied in [18], which leads to a nonlinear Black Scholes (BS) equation in the form (2.1) with g the option payoff and an Hamiltonian H given on $(0, \infty) \times \mathbb{R}$ by

$$H(x, \gamma) = \begin{cases} \frac{1}{2}\sigma^2 \frac{x^2\gamma}{1-\lambda x^2\gamma}, & \text{if } \lambda x^2\gamma < 1 \\ \infty, & \text{otherwise.} \end{cases} \quad (5.3)$$

where $\sigma > 0$ is the volatility in the BS model, and λ is a nonnegative constant related to the linear market impact. Notice that H can be written in Bellman form as

$$H(x, \gamma) = \sup_{a \geq 0} \left[\frac{1}{2}ax^2\gamma - \frac{1}{2\lambda}(\sqrt{a} - \sigma)^2 \right],$$

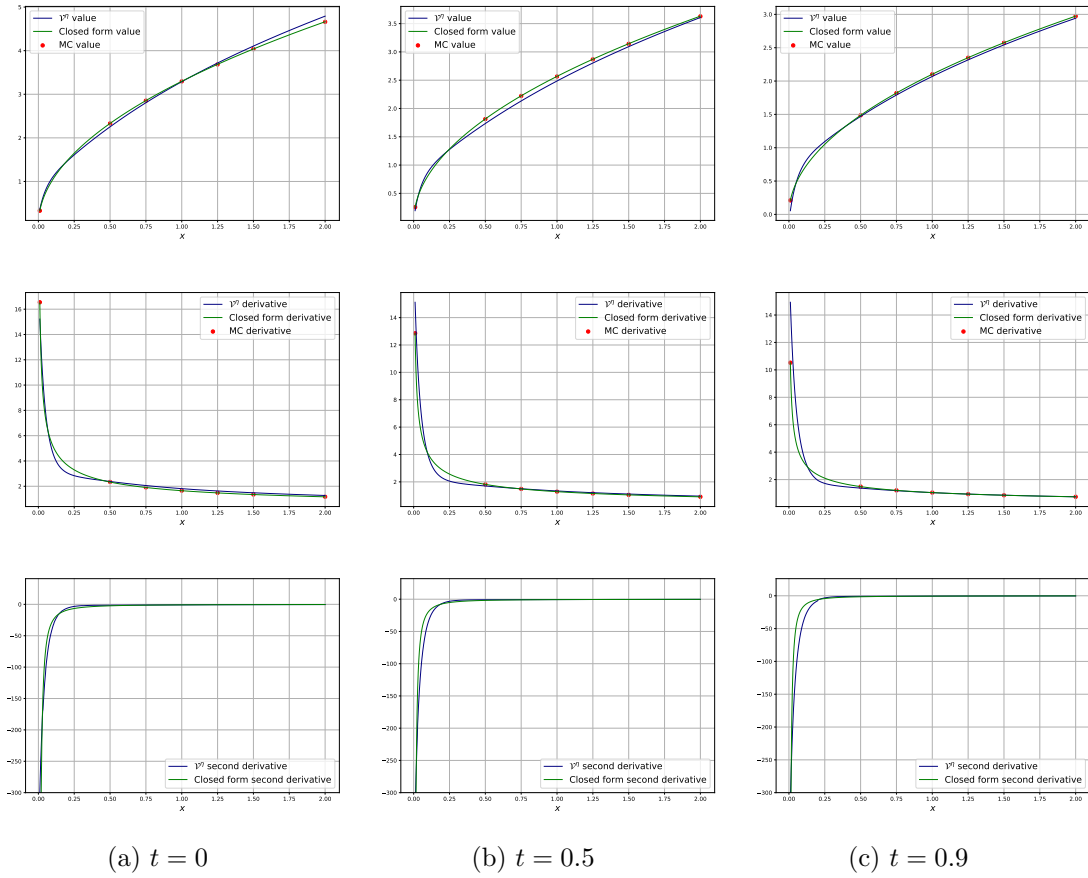


Figure 3: Value function v^{γ} and its first and second derivative obtained by Differential regression Learning (Algorithm 2) for the Merton problem with parameters $b = 0.2$, $\sigma = 0.2$ and power utility with exponent $\gamma = 0.5$, plotted as functions of x , for fixed values of t .

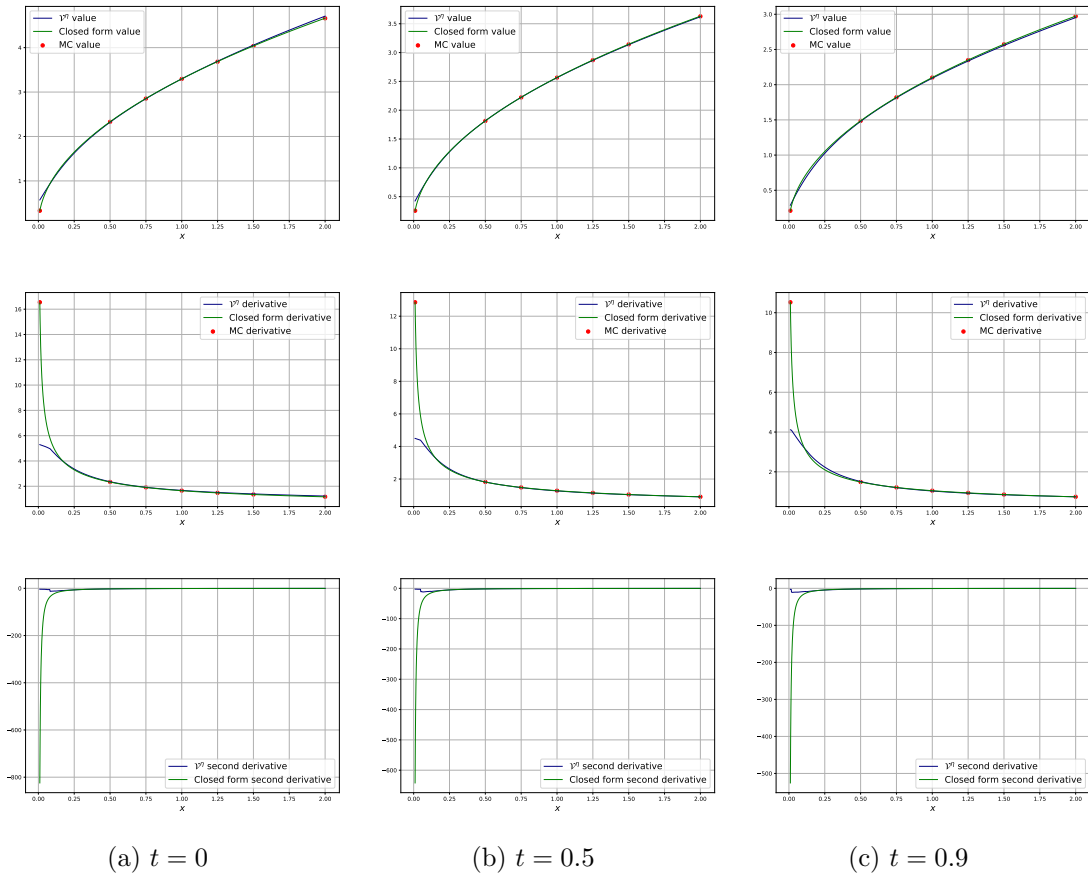


Figure 4: Value function v^γ and its first and second derivative obtained by Pathwise learning (Algorithm 3) for the Merton problem with parameters $b = 0.2$, $\sigma = 0.2$ and power utility with exponent $\gamma = 0.5$, plotted as functions of x , for fixed values of t .

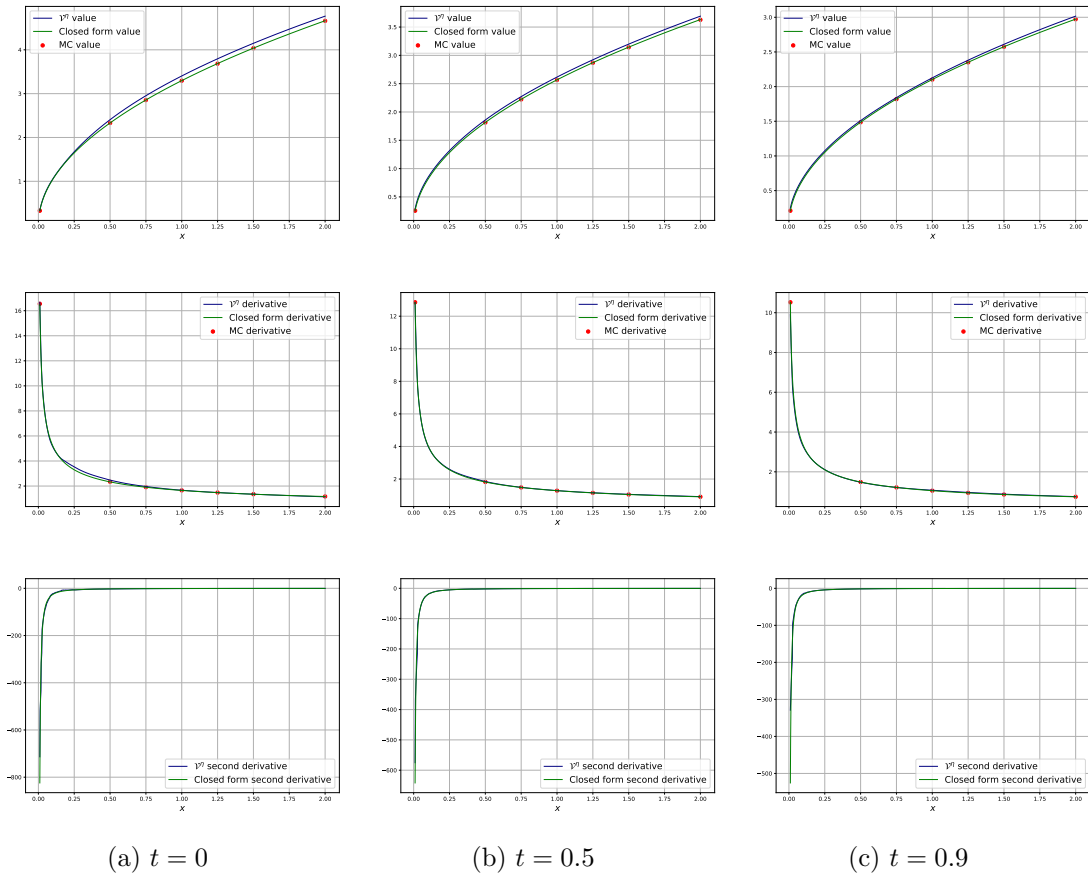


Figure 5: Value function v^{γ} and its first and second derivative obtained by Pathwise differential learning (Algorithm 4) for the Merton problem with parameters $b = 0.2$, $\sigma = 0.2$ and power utility with exponent $\gamma = 0.5$, plotted as functions of x , for fixed values of t .

which corresponds to the dual stochastic control representation of the option price u as

$$u(t, x) = \sup_{\alpha} \mathbb{E} \left[g(X_T^{t,x,\alpha}) - \frac{1}{2\lambda} \int_t^T (\sqrt{\alpha_s} - \sigma)^2 ds \right], \quad (5.4)$$

where $X = X^{t,x,\alpha}$ is governed by the controlled dynamics

$$dX_s = X_s \sqrt{\alpha_s} dW_s, \quad t \leq s \leq T, \quad X_t = x > 0,$$

with a control process α valued in \mathbb{R}_+ .

We shall apply the various differential learning methods to this problem for two examples of option payoff.

5.6.1 Closed-form solution for a logarithmic terminal cost

We first consider the toy example where the option payoff g is logarithmic: $g(x) = \ln x$. Indeed, in this case, we can check that the solution to the pricing PDE (2.1) with H as in (5.3) is given in closed-form by

$$u(t, x) = \ln(x) - \frac{\sigma^2}{2(1+\lambda)}(T-t),$$

while the optimal control to the dual stochastic control representation (5.4) is constant equal to

$$\hat{\alpha}(t, x) = \left(\frac{\sigma}{1+\lambda} \right)^2.$$

In order to check that the value function approximation obtained is a lower bound of the true one, we compute in Table 3 the difference between the closed form value function and the estimation of the value function on points (t, x) obtained by computing the expectation (2.5) by Monte Carlo on $1e^6$ trajectories controlled by the Deep Learning approximation of the optimal control. We compute the value functions on a grid $t \in \{0, 0.5, 0.9\}$, $x \in \{1e^{-2}, 0.5, 0.75, 1, 1.25, 1.5, 2\}$ with parameter $\sigma = 0.3$ and linear market impact factor $\lambda = 5e^{-3}$ and present in the table the difference between the closed form value and the Monte Carlo approximation. For clarity of presentation we present the results averaged over t in this table.

In Table 4, we compute the residual losses defined in (5.2) for the NN ϑ^η obtained by the various deep learning methods: the differential learning scheme (Algorithm 2), the pathwise martingale learning with 1 NN (Algorithm 3), the pathwise differential learning with 1 NN (Algorithm 4). We also provide the training time for 500 epochs for each of these algorithms. On this table, we see that the Pathwise learning methods yield better results than the Differential regression learning methods. The difference between the residual loss

	$x = 1e^{-2}$	$x = 0.5$	$x = 0.75$	$x = 1$	$x = 1.25$	$x = 1.5$	$x = 2$
Difference closed - MC	$2.673e^{-4}$	$2.042e^{-4}$	$2.058e^{-4}$	$2.066e^{-4}$	$2.099e^{-4}$	$2.147e^{-4}$	$2.300e^{-4}$

Table 3: Difference between the closed form value function and the value computed by Monte Carlo on $1e^6$ trajectories on points $x \in \{1e^{-2}, 0.5, 0.75, 1, 1.25, 1.5, 2\}$ and averaged over times $t \in \{0, 0.5, 0.9\}$ for Black-Scholes problem with linear market impact factor $\lambda = 5e^{-3}$ and parameter $\sigma = 0.3$.

	Diff. regr. learning	Path. 1NN	Path. diff. 1NN
Residual loss	$2.046e^{-3}$	$3.484e^{-4}$	$6.644e^{-4}$
Residual loss + terminal loss	$2.179e^{-3}$	$3.864e^{-4}$	$6.758e^{-4}$
Training time (500 epochs)	163s	130s	525s

Table 4: Residual and boundary losses computed on a 102x102 time and space grid with $t \in [0, 0.9]$ and $x \in [0.1, 2]$ for a terminal logarithmic payoff, with parameter $\sigma = 0.3$ and linear market impact factor $\lambda = 5e^{-3}$.

only and the sum of the residual and terminal loss is small in all three methods, meaning that both the PDE solution’s derivatives and terminal condition have been learned by the neural network.

We plot the value function $\vartheta^\eta(t, x)$ and its derivatives $\partial_x \vartheta^\eta(t, x)$ and $\partial_{xx} \vartheta^\eta(t, x)$ for fixed values $t = 0, t = 0.5, t = 0.9$, parameter $\sigma = 0.3$ and linear market impact factor $\lambda = 5e^{-3}$, and compare it with the closed-form solution of the problem. Figure 6 corresponds to the Differential regression learning method, Figure 7 corresponds to the pathwise martingale learning while Figure 8 corresponds to the pathwise differential learning method. On these graphs, we can see that the three methods, as well as the Monte-Carlo values ϑ_{MC} and $D_x \vartheta_{MC}$, yield good approximations of the PDE solution and its derivatives. Notice however that the pathwise learning (see Figure 7) does not provide a good approximation of the second derivative on the boundary points of the grid, namely the points that were not explored by the simulations, but when combining with the differential learning (see Figure 8), it greatly improves the approximation of the second derivative.

5.6.2 Call-option type terminal condition

We now consider a usual call option payoff with strike $K = 1$, hence a function g equal to: $g(x) = \max(x - 1, 0)$.

Again, we compute in Table 5, the residual losses defined in (5.2) for the NN ϑ^η obtained by the various deep learning methods: the differential learning scheme (Algorithm 2),

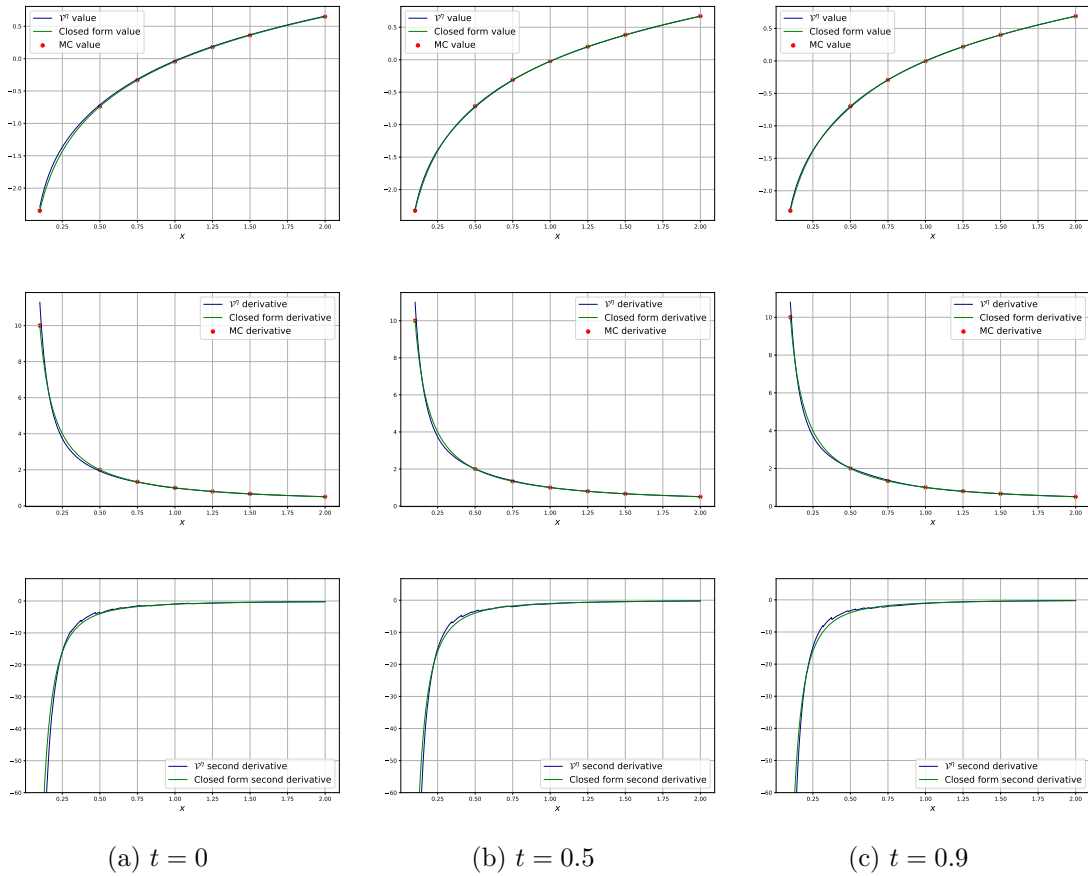


Figure 6: Value function v^{η} and its first and second derivative obtained by Differential Regression Learning (Algorithm 2) for a logarithmic option payoff, with parameter $\sigma = 0.3$ and linear market impact factor $\lambda = 5e^{-3}$, plotted as functions of x , for fixed values of t .

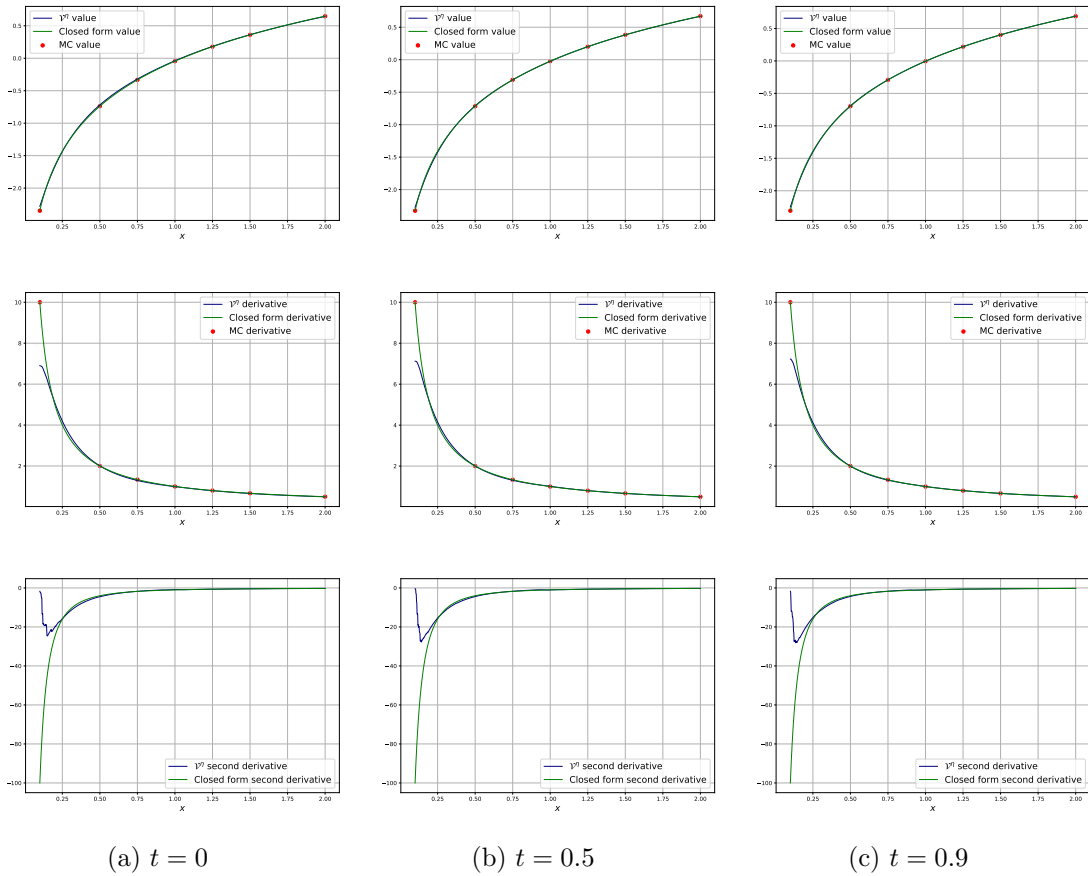


Figure 7: Value function v^γ and its first and second derivative obtained by Pathwise Learning (Algorithm 3) for a logarithmic option payoff, with parameter $\sigma = 0.3$ and linear market impact factor $\lambda = 5e^{-3}$, plotted as functions of x , for fixed values of t .

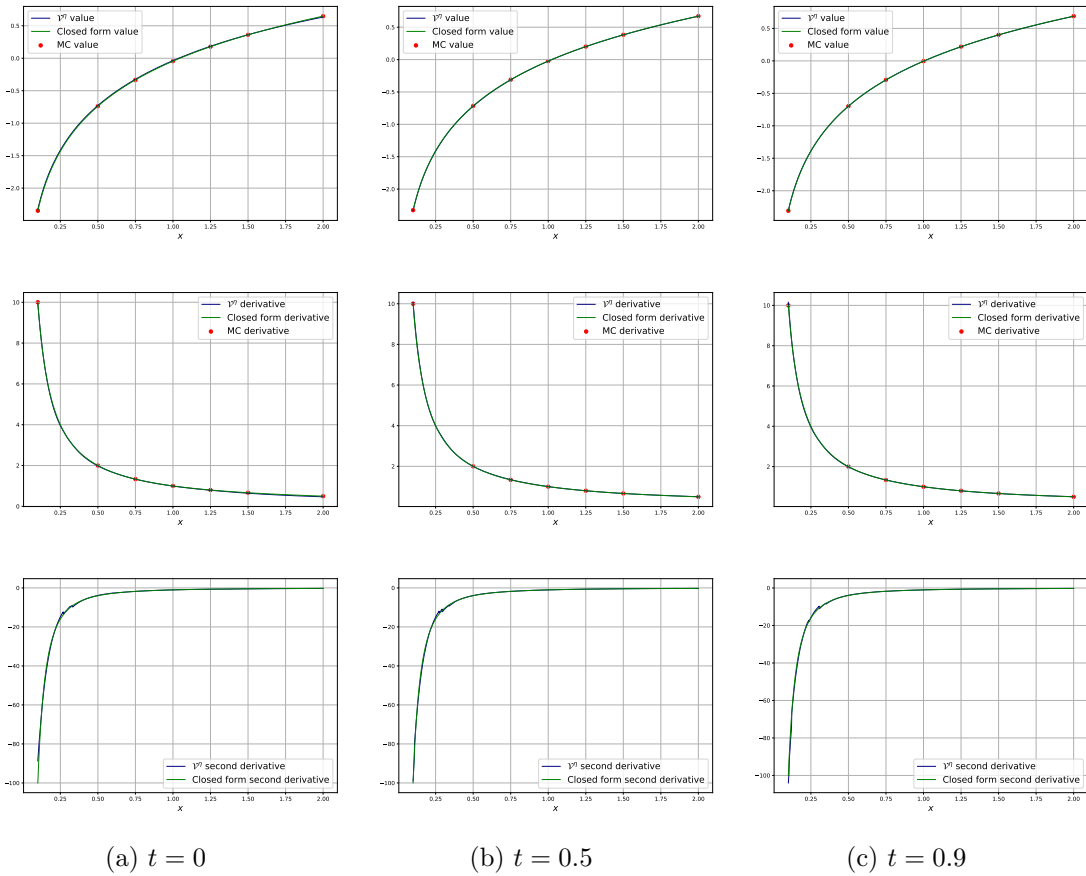


Figure 8: Value function v^0 and its first and second derivative obtained by Pathwise Differential Learning (Algorithm 4) for a logarithmic option payoff, with parameter $\sigma = 0.3$ and linear market impact factor $\lambda = 5e^{-3}$, plotted as functions of x , for fixed values of t .

the pathwise martingale learning with 1 NN (Algorithm 3) and the pathwise differential learning with 1 NN (Algorithm 4). We also provide the training time for each of these algorithms. On this table, we see that the Differential regression learning and the Pathwise differential methods yield better results than the "simple" Pathwise method. Despite having the lowest residual loss, the Pathwise method gives the biggest terminal loss. This shows that, while the time and second space derivatives of the neural network give a low residual loss corresponding to the Hamiltonian (5.3), the network does not manage to fit the terminal function. This phenomenon is also present, to a lesser extent, in the approximation given by the Differential regression learning method. Out of the three methods, the Pathwise differential yields the smallest residual and terminal losses.

	Diff. regr. learning	Path. 1NN	Path. diff. 1NN
Residual loss	$2.998e^{-4}$	$2.756e^{-4}$	$2.283e^{-4}$
Residual loss + terminal loss	$3.972e^{-4}$	$1.004e^{-3}$	$2.538e^{-4}$
Training time	262s 1000 epochs	299s 1000 epochs	584s 500 epochs

Table 5: Residual and boundary losses computed on a 102x102 time and space grid with $t \in [0, 0.9]$ and $x \in [0.1, 2]$ for a terminal call-option payoff $g(x) = \max(x - 1, 0)$, with parameter $\sigma = 0.3$ and linear market impact factor $\lambda = 5e^{-3}$.

We plot again the value function $\vartheta^\eta(t, x)$ and its derivative $\partial_x \vartheta^\eta(t, x)$ for fixed values $t = 0$, $t = 0.5$, $t = 0.9$, parameter $\sigma = 0.3$ and linear market impact factor $\lambda = 5e^{-3}$, and compare it with the Monte-Carlo estimation obtained. The Figure 9 corresponds to the Differential regression learning method, Figure 10 corresponds to the pathwise martingale learning while Figure 11 corresponds to the Pathwise differential learning method. Graphically, the results of the Differential regression learning and the Pathwise differential learning methods are very close to the points obtained by Monte Carlo estimation for the value and the first derivative. The Pathwise methods does not give a good approximation of the value and the derivatives for values of x smaller than 1. The difference of performance between the Pathwise and the Differential pathwise methods is analogous to the one observed between Differential regression learning and "simple" regression learning in Figure 1, demonstrating the interest of adding a regression term for the derivative of the neural network.

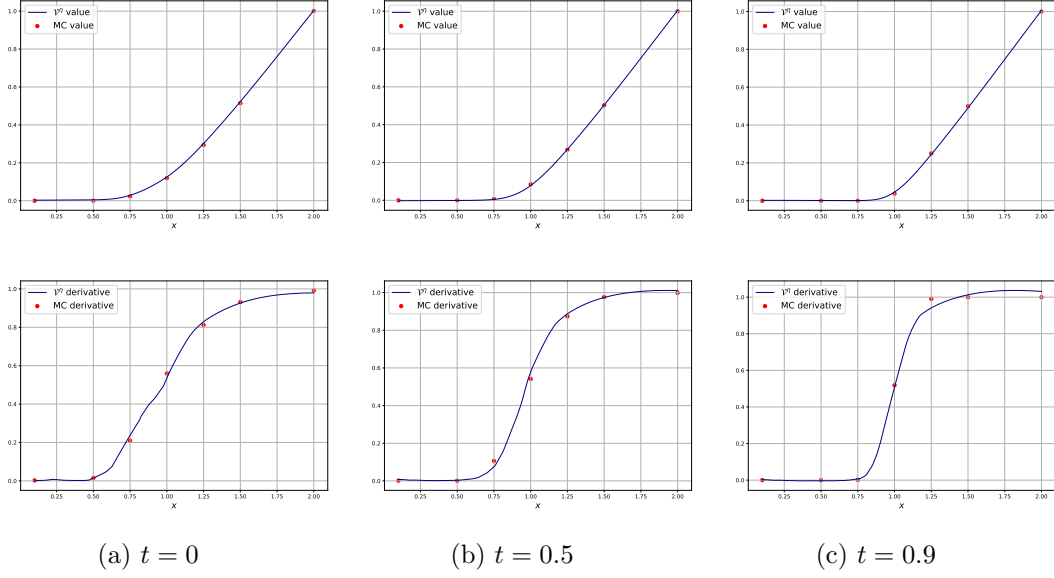


Figure 9: Value function ϑ^η and its derivative obtained by Differential Regression Learning (Algorithm 2) for a call option with strike 1, with parameter $\sigma = 0.3$ and linear market impact factor $\lambda = 5e^{-3}$, plotted as functions of x , for fixed values of t .

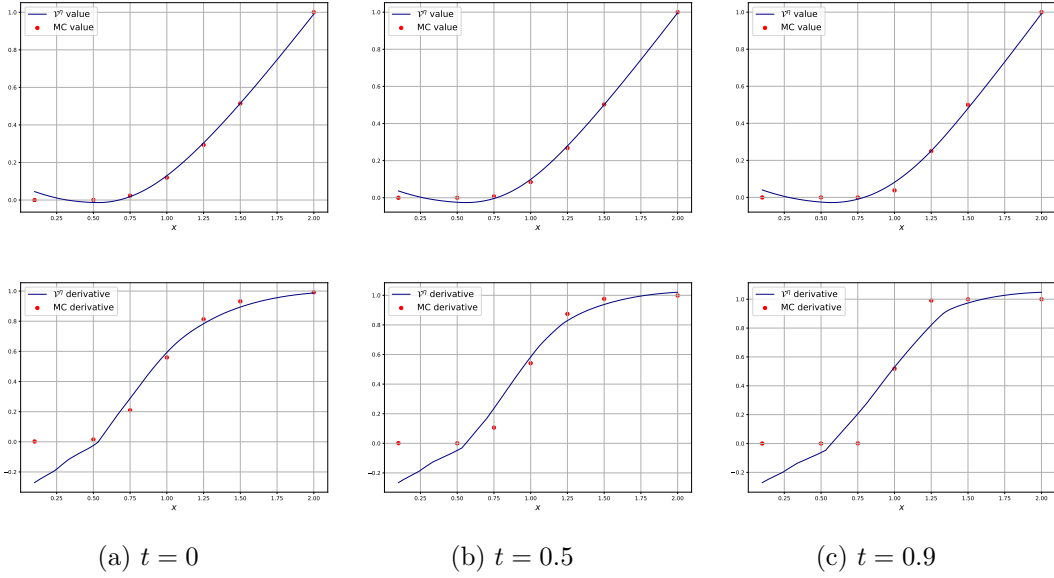


Figure 10: Value function ϑ^η and its derivative obtained by Pathwise Learning (Algorithm 3) for a call option with strike 1, with parameter $\sigma = 0.3$ and linear market impact factor $\lambda = 5e^{-3}$, plotted as functions of x , for fixed values of t .

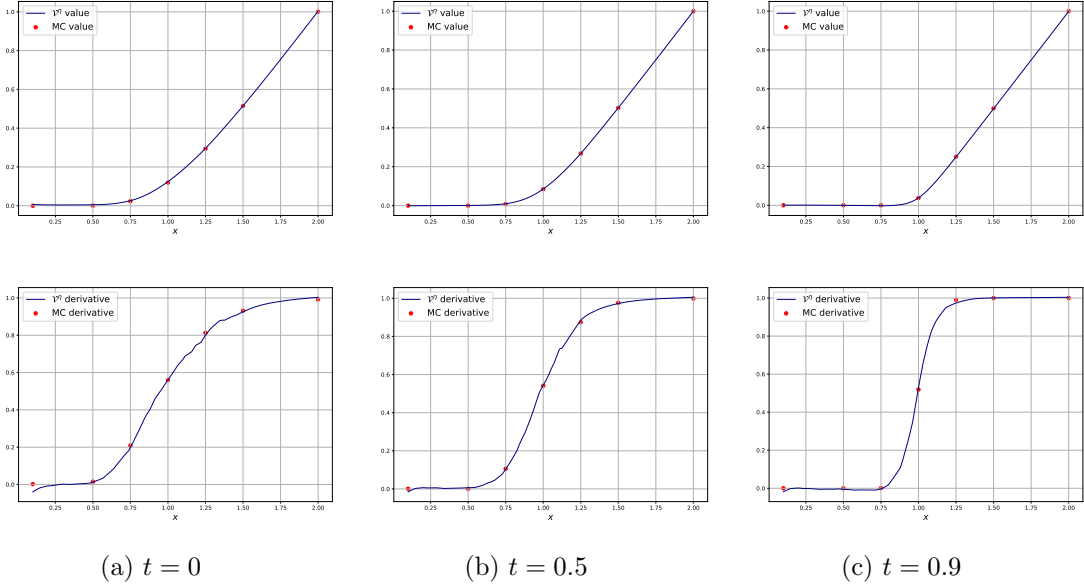


Figure 11: Value function ϑ^η and its derivative obtained by Pathwise Differential Learning (Algorithm 4) for a call option with strike 1, with parameter $\sigma = 0.3$ and linear market impact factor $\lambda = 5e^{-3}$, plotted as functions of x , for fixed values of t .

6 Further step: resolution for parametric terminal functions

6.1 Theory and network structure

In line with the works in [34], [10], [29], our next goal is to design a Machine Learning method allowing us to directly obtain a solution of problem (2.3) for a parametric terminal condition g_K , for every value of the parameter $K \in \mathbb{R}^p$ in a compact set. In other words, we aim to learn the operator that maps the payoff function parameter K to the solution of the PDE with terminal condition g_K . We want to be able to train the neural networks once and for all on a selection of parameter values and obtain a network which takes a couple (t, x) and the parameter value K and outputs the solution of the problem. In [10] the authors solve parametric PDEs by using a variant of highway networks [32], which are feedforward networks where each dense layer has an additional parameter called *gate* which allows the layer to output a combination of the unmodified input and of the output of the affine and activation operations, alleviating the vanishing gradient problem and allowing to train deeper networks. Their network takes the time, space and PDE parameter as input and is trained in the spirit of the Deep Galerkin method. The PDE residuals is computed from the neural network on a random time, space and parameter grid and is minimized in order to approximate the PDE solution. In [34] the authors give four methods to solve parametric

PDEs using a fully connected network taking the time, space and PDE parameter as input and minimizing a loss averaged over random parameter values. In this article we follow the methodology developed in [29] by relying on a class of neural networks, called DeepONet, presented in [20], and aiming to approximate functional operators. This method is based on the following universal approximation theorem for operator, due to Chen and Chen [5].

Theorem 6.1. *Suppose that σ is a continuous non-polynomial function, X is a Banach space, $K_1 \subset X$, $K_2 \subset \mathbb{R}^d$ are two compact sets in X and \mathbb{R}^d , respectively, V is a compact set in $C(K_1)$, G is a nonlinear continuous operator, which maps V into $C(K_2)$. Then for any $\epsilon > 0$, there are positive integers n, p, m , constants $c_i^k, \xi_{ij}^k, \theta_i^k, \zeta_k \in \mathbb{R}$, $w_k \in \mathbb{R}^d$, $x_j \in K_1, i = 1, \dots, n, k = 1, \dots, p, j = 1, \dots, m$, such that*

$$\left\| G(u)(y) - \underbrace{\sum_{k=1}^p \sum_{i=1}^n c_i^k \sigma \left(\sum_{j=1}^m \xi_{ij}^k u(x_j) + \theta_i^k \right)}_{\text{branch net}} \underbrace{\sigma(w_k y + \zeta_k)}_{\text{trunk net}} \right\| < \epsilon,$$

holds for all $u \in V$ and $y \in K_2$.

The network used in [20] is composed of two sub networks, the *branch net*, which takes the terminal function estimated on a fixed number of points called *sensors* as input, and the *trunk net*, which takes the time and space coordinates as input. In our case, as in [29], the *branch net* takes the parametric terminal function estimated on a grid of *sensors*, and will be trained for random values of the function's parameter. We represent the structure of this neural network in Figure 12.

As our numerical methods proceed in two stages, by first approximating the optimal control of problem (2.3) with a neural network and then approximating the associated value function with another network, we again use a DeepONet to approximate the optimal control and then another one to approximate the value function u by differential learning.

While the authors of [20] train a DeepONet in a supervised manner, we train our network in an **unsupervised way**.

As before, we start by training the control network a_θ in order to approximate the optimal control of problem. We use a batch of M independent trajectories $\{x_{t_n}^{m, K_m, \theta}, t_n \in \mathcal{T}_N\}$, $m = 1, \dots, M$, of $\{X_{t_n}^{K_m, \theta}, t_n \in \mathcal{T}_N\}$, where the K superscript denotes that the trajectory is driven by a control with input parameter K , and M random parameter values K_m randomly sampled from a distribution μ_K with compact support in \mathbb{R}^p , and apply a stochastic gradient ascent method to the empirical gain function:

$$J_M(\theta) = \frac{1}{M} \sum_{m=1}^M \left[g(x_T^{m, K_m, \theta}, K_m) + \sum_{n=0}^{N-1} f(x_{t_n}^{m, K_m, \theta}, a_\theta(t_n, x_{t_n}^{m, K_m, \theta}, K_m)) \Delta t_n \right].$$

The pseudo-code is described in Algorithm 5. The output of this algorithm yields a parameter θ^* , and so an approximation of the optimal feedback control with $a^* = a_{\theta^*}$, and of

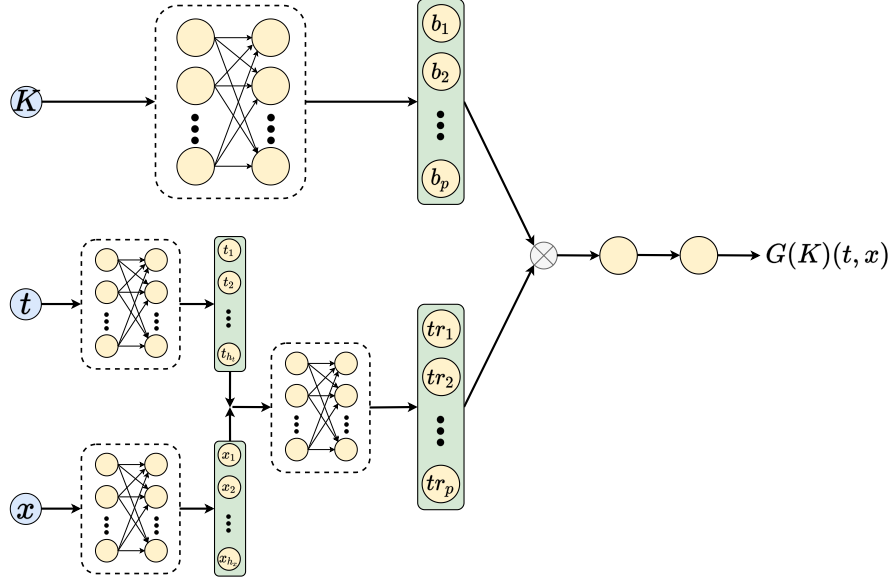


Figure 12: Structure of the DeepONet network.

the associated optimal state process with $X^* = X^{\theta^*}$. In the sequel, to alleviate notations, we shall omit the superscript $*$, and simply denote a and X .

From this optimal control approximation, the value function is then approximated through the Differential regression learning algorithm presented in Section 5.2 modified in order to train the network for different values of the terminal function parameter K . The target payoff and its derivative are then computed as

$$Y_T^{K_m, t_n} = g(X_T^{K_m}, K_m) + \sum_{q=n}^{N-1} f^{a^*}(t_q, X_{t_q}^{K_m}) \Delta t_q, \quad n = 0, \dots, N,$$

$$Z_T^{K_m, t_n} = (D_{X_{t_n}} X_T^{K_m})^\top D_x g(X_T^{K_m}, K_m) + \sum_{q=n}^{N-1} (D_{X_{t_n}} X_{t_q}^{K_m})^\top D_x f^{a^*}(t_q, X_{t_q}^{K_m}) \Delta t_q,$$

with the convention that the above sum over q is zero when $n = N$. For the training of the neural network ϑ^η , we use a batch of M independent samples $(x_{t_n}^{m, K_m}, y_T^{m, K_m, t_n}, z_T^{m, K_m, t_n})$, $m = 1, \dots, M$, of $(X_{t_n}^{K_m}, Y_T^{K_m, t_n}, Z_T^{K_m, t_n})$, $n = 0, \dots, N$ and M random parameter values K^m randomly sampled from a distribution μ_K with compact support in \mathbb{R}^p , and apply

Algorithm 5: Deep learning scheme to solve the stochastic control problem (2.3)

Result: A set of optimized parameters θ^* ;
 Initialize the learning rate l and the neural network \mathfrak{a}_θ ;
 Generate an \mathbb{R}^{N+1} -valued time grid $0 = t_0 < t_1 < \dots < t_N = T$ with time steps $(\Delta t_n)_{n=0, \dots, N-1}$;
 Generate a batch of M starting points $X_0 \sim \mu_0$, Brownian increments $(\Delta W_{t_n})_{n=0, \dots, N-1}$ in \mathbb{R}^d and parameter values $K \sim \mu_K$;
for each batch element m do
 Compute the trajectory $(x_{t_n}^{m, K_m, \theta})_{n=0, \dots, N}$ through the scheme

$$x_{t_{n+1}}^{m, K_m, \theta} = x_{t_n}^{m, K_m, \theta} + \mathfrak{b}(x_{t_n}^{m, K_m, \theta}, \mathfrak{a}_\theta(t_n, x_{t_n}^{m, K_m, \theta}, K_m))\Delta t_n + \sigma(x_{t_n}^{m, K_m, \theta}, \mathfrak{a}_\theta(t_n, x_{t_n}^{m, K_m, \theta}, K_m))\Delta w_{t_n}^m,$$

 from the generated starting point $x_{t_0}^m$, Brownian increments $(\Delta w_{t_n}^m)_{n=0, \dots, N-1}$ and parameter K_m ;
end
for each epoch do
 Compute the batch loss

$$J_M(\theta) = \frac{1}{M} \sum_{m=1}^M \left[g(x_T^{m, K_m, \theta}, K_m) + \sum_{n=0}^{N-1} f(x_{t_n}^{m, K_m, \theta}, \mathfrak{a}_\theta(t_n, x_{t_n}^{m, K_m, \theta}, K_m))\Delta t_n \right]$$

 Compute the gradients $\nabla_\theta J_M(\theta)$;
 Update $\theta \leftarrow \theta - l \nabla_\theta J_M(\theta)$;
end
Return: The set of optimized parameters θ^* ;

stochastic gradient descent for the minimization of the mean squared error functions

$$MSE_{val}(\eta) = \frac{1}{M} \sum_{m=1}^M \sum_{n=0}^{N-1} |y_T^{m, K_m, t_n} - \vartheta^\eta(t_n, x_{t_n}^{m, K_m}, K_m)|^2 \Delta t_n$$

$$MSE_{der}(\eta) = \frac{1}{M} \sum_{m=1}^M \sum_{n=0}^{N-1} \frac{1}{\|z_T^{K_m, t_n}\|^2} |z_T^{m, K_m, t_n} - D_x \vartheta^\eta(t_n, x_{t_n}^{m, K_m}, K_m)|^2 \Delta t_n.$$

The pseudo-code is described in Algorithm 6.

Algorithm 6: Deep learning scheme for Differential Regression learning

Result: A set of optimized parameters η^* ;
Initialize the learning rate l , the neural networks ϑ^η ;
Generate an \mathbb{R}^{N+1} -valued time grid $0 = t_0 < t_1 < \dots < t_N = T$ with time steps $(\Delta t_n)_{n=0, \dots, N-1}$;
Generate a batch of M starting points $X_0 \sim \mu_0$, Brownian increments $(\Delta W_{t_n})_{n=0, \dots, N}$ in \mathbb{R}^d and parameter values $K \sim \mu_K$;
for each batch element m **do**
 Compute the trajectory $(x_{t_n}^{m, K_m})_{n=0, \dots, N}$ through the scheme

$$x_{t_{n+1}}^{m, K_m} = x_{t_n}^{m, K_m} + b^{a^*}(t_n, x_{t_n}^{m, K_m})\Delta t_n + \sigma^{a^*}(t_n, x_{t_n}^{m, K_m})\Delta w_{t_n}^m,$$

 from the generated starting point $x_{t_0}^m$, Brownian increments $(\Delta w_{t_n}^m)_{n=0, \dots, N-1}$, parameter K_m and previously trained control $a = a_{\theta^*}$;
 Compute the value and derivative targets $(y_T^{m, K_m, t_n})_{n=0, \dots, N}$ and $(z_T^{m, K_m, t_n})_{n=0, \dots, N}$;
end
for each epoch **do**
 if Epoch number is even **then**
 Compute, for every batch element m , the integral $\sum_{n=0}^{N-1} |y_T^{m, K_m, t_n} - \vartheta^\eta(t_n, x_{t_n}^{m, K_m}, K_m)|^2 \Delta t_n$;
 Compute the batch loss $MSE_{val}(\eta)$;
 Compute the gradient $\nabla_\eta MSE_{val}(\eta)$;
 Update $\eta \leftarrow \eta - l \nabla_\eta MSE_{val}(\eta)$;
 end
 else
 Compute, for every batch element m , the integral $\sum_{n=0}^{N-1} |z_T^{m, K_m, t_n} - D_x \vartheta^\eta(t_n, x_{t_n}^{m, K_m}, K_m)|^2 \Delta t_n$;
 Compute the batch loss $MSE_{der}(\eta)$;
 Compute the gradient $\nabla_\eta MSE_{der}(\eta)$;
 Update $\eta \leftarrow \eta - l \nabla_\eta MSE_{der}(\eta)$;
 end
end
Return: The set of optimized parameters η^* ;

6.2 Application to the Black-Scholes model with linear market impact

Using this DeepONet based algorithm, we revisit the resolution of the nonlinear Black Scholes equation presented in Section 5.6. In this Section, we use the Algorithms 5 and 6 in order to solve the PDE for a terminal function corresponding to a call option payoff $g(x, K) = \max(x - K, 0)$ with parameter (or *strike*) $K \in \mathbb{R}_+^*$.

The *branch net* of the **DeepONet used to approximate the control** as a function of the terminal function g_K is a standard feed-forward network composed of two layers with 50 neurons and use the *tanh* activation function. The *trunk net* has the same structure as the network used in the previous sections and represented in Figure 2. It is composed of two sub-networks taking respectively the time t and state x as an input and each composed of two layers of 50 neurons using the *tanh* activation function. The outputs of these two sub-networks are concatenated into a vector of \mathbb{R}^{100} which passes through two additional layers of 50 neurons using *tanh* activation. The output of the *branch net* and the *trunk net*, which have the same dimension, are then combined through a dot product whose output

passes through a layer of one neuron using \tanh activation and a layer of one neuron using the *Parametric ReLU* activation function ensuring, as explained in Section 5.1, that the control obtained belongs to the control space A .

The **DeepONet used to approximate the value function** u shares the same structure. The branch and trunk net have the same structures as the ones used in the control DeepONet with the same number of layers and neurons per layer and with *Swish* activation function, defined as

$$\text{Swish}(x) = \frac{x}{1 + e^{-x}}.$$

After the dot product, the output also passes through a layer composed of one neuron using *Swish* activation function and a last layer of one neuron using no activation function.

Remark 6.2. *For the control DeepONet, we used the \tanh activation function instead of the ELU activation used in the previous sections as we encountered loss divergences during the training of the DeepONet with ELU activation. Since the \tanh activation is bounded, the problem was resolved using this function.*

For the value DeepONet, we used the Swish activation function instead of the ELU activation used in the previous sections as it empirically gave better results. As the ELU function's second derivative is discontinuous, a kink was observed on the value function's derivative we obtained with the DeepONet. This effect was not present when performing the "simple" regression with a standard network in the previous sections, probably because the regression problem is simpler and the true value function fitted with a better accuracy. Since the Swish activation is of class C^∞ , we obtained better results, without kinks, using this function.

For both trainings, we use the Adam optimizer with a learning rate equal to $1e^{-3}$ and train the network on 8192 random trajectories and strike values. In order to test the generalization power of our method, we train the control and value neural networks on strikes randomly sampled from $\mathcal{U}([0.25, 0.75] \cup [1.5, 2])$ and test the network on strikes chosen in $[0.2, 2.1]$. We plot in figure 13 below the optimal control approximation obtained along for $K = 1$ along with the control approximation obtained by Algorithm 1 (denoted *regular network control*) which serves as a reference.

We compute in Table 6, the residual losses defined in (5.2) for the DeepONet ϑ^η by the Differential Regression Learning scheme (Algorithm 6). We compute the residual losses on a 102×102 linearly spaced time and space grid with $t \in [0, 0.9]$ and $x \in [0, 3]$ for a terminal call option payoff for strikes $K \in \{0.2, 0.5, 1, 1.75, 2, 2.1\}$, with parameter $\sigma = 0.3$ and linear market impact factor $\lambda = 5e^{-3}$.

We plot below the value function $\vartheta^\eta(t, x)$ and its derivative $\partial_x \vartheta^\eta(t, x)$ obtained by Differential Regression Learning with DeepONet networks, for fixed values $t = 0$, $t = 0.5$, $t = 0.9$, parameter $\sigma = 0.3$ and linear market impact factor $\lambda = 5e^{-3}$, and compare it with

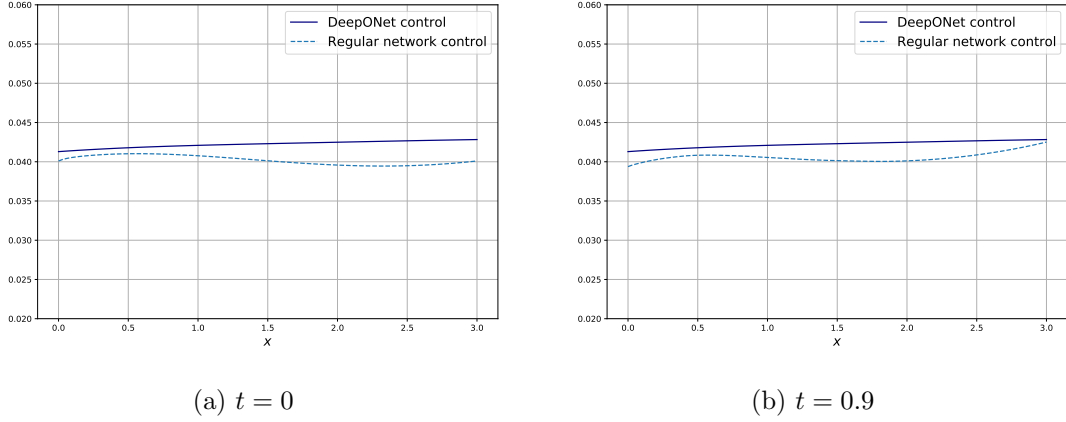


Figure 13: Control a_θ obtained by global method with DeepONet (Algorithm 5) for a call option with strike $K = 1$, with parameter $\sigma = 0.3$ and linear market impact factor $\lambda = 5e^{-3}$, plotted as functions of x , for fixed values of t .

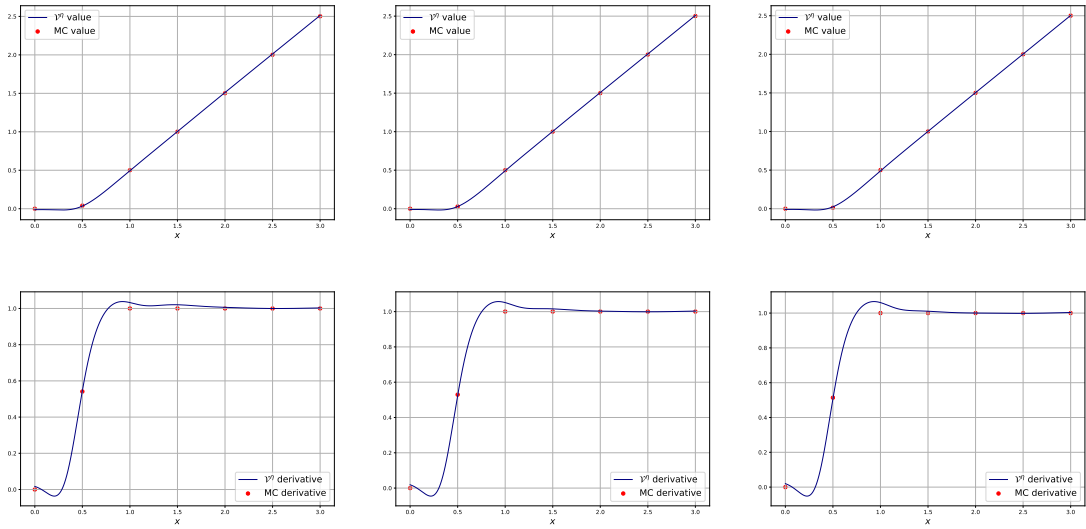


Figure 14: Value function ϑ^η (first line) and its derivative (second line) obtained by Differential Regression Learning (Algorithm 6) for a terminal call option payoff with strike $K = 0.5$, with parameter $\sigma = 0.3$ and linear market impact factor $\lambda = 5e^{-3}$, plotted as functions of x , for fixed values of t .

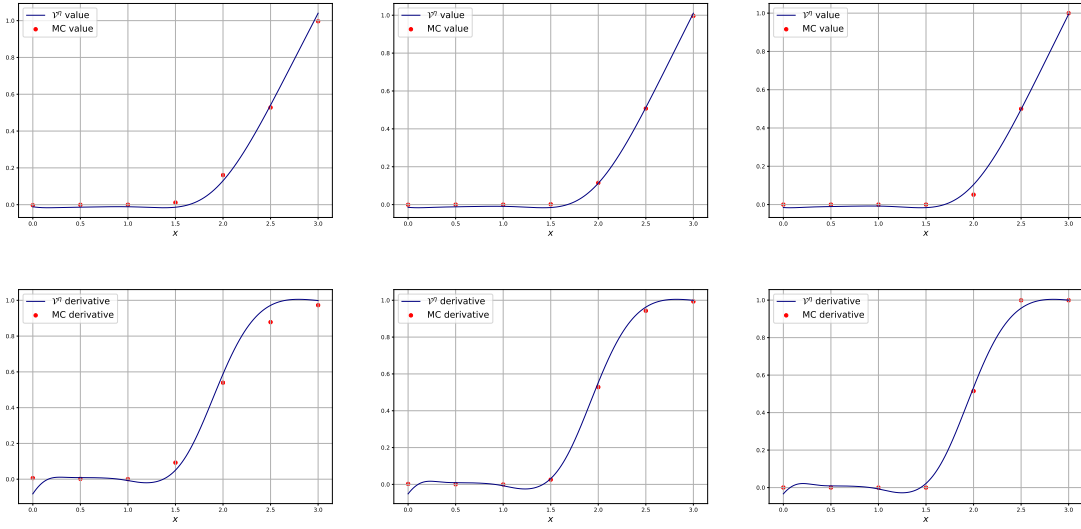


Figure 15: Value function ϑ^η (first line) and its derivative (second line) obtained by Differential Regression Learning (Algorithm 6) for a terminal call option payoff with strike $K = 2$, with parameter $\sigma = 0.3$ and linear market impact factor $\lambda = 5e^{-3}$, plotted as functions of x , for fixed values of t .

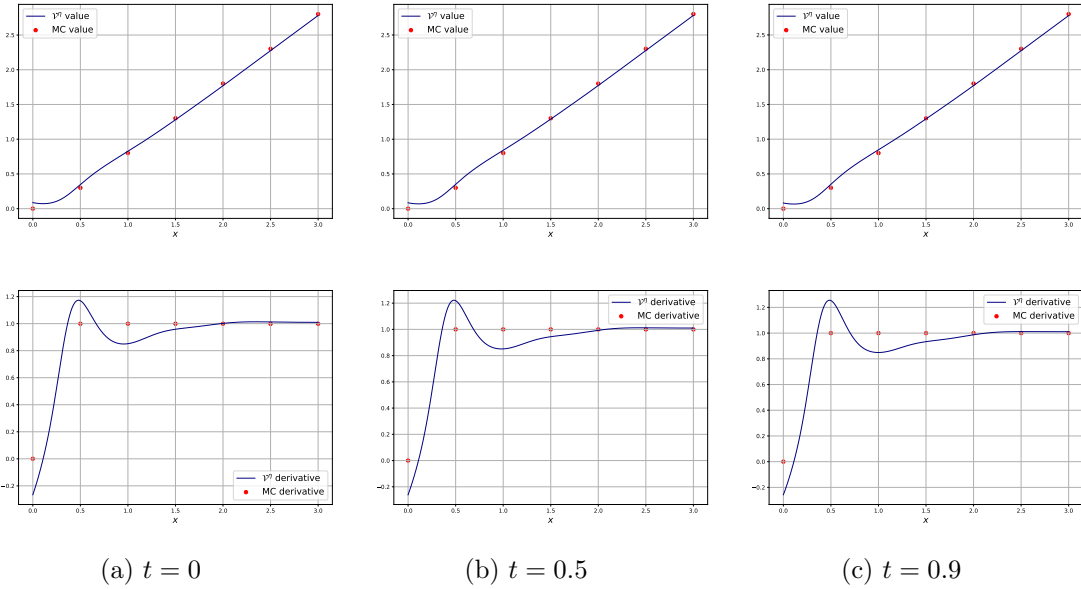


Figure 16: Value function ϑ^η (first line) and its derivative (second line) obtained by Differential Regression Learning (Algorithm 6) for a terminal call option payoff with strike $K = 0.2$, with parameter $\sigma = 0.3$ and linear market impact factor $\lambda = 5e^{-3}$, plotted as functions of x , for fixed values of t .

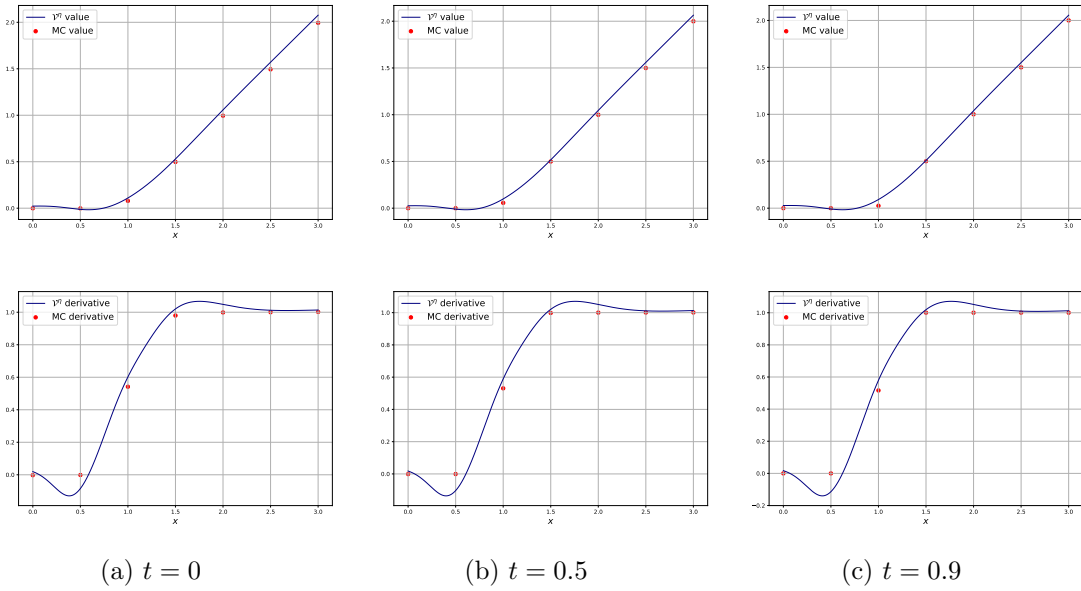


Figure 17: Value function ϑ^η (first line) and its derivative (second line) obtained by Differential Regression Learning (Algorithm 6) for a terminal call option payoff with strike $K = 1$, with parameter $\sigma = 0.3$ and linear market impact factor $\lambda = 5e^{-3}$, plotted as functions of x , for fixed values of t .

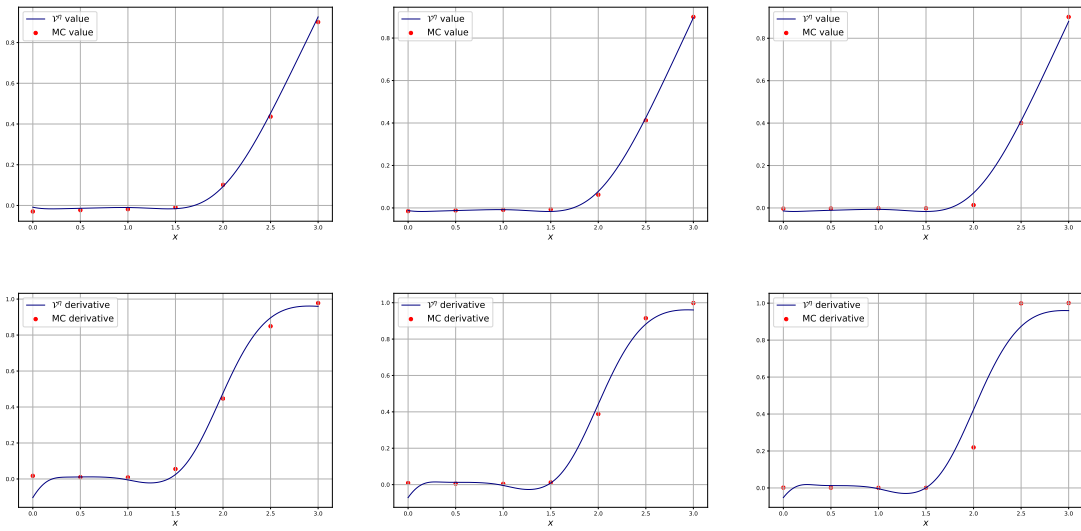


Figure 18: Value function ϑ^η (first line) and its derivative (second line) obtained by Differential Regression Learning (Algorithm 6) for a terminal call option payoff with strike $K = 2.1$, with parameter $\sigma = 0.3$ and linear market impact factor $\lambda = 5e^{-3}$, plotted as functions of x , for fixed values of t .

	$K = 0.2$	$K = 0.5$	$K = 1$	$K = 1.75$	$K = 2$	$K = 2.1$
Residual loss + terminal loss	$1.918e^{-3}$	$1.461e^{-4}$	$1.700e^{-3}$	$1.162e^{-3}$	$2.002e^{-3}$	$2.175e^{-3}$

Table 6: Residual and boundary losses computed on a 102x102 time and space grid with $t \in [0, 0.9]$ and $x \in [0, 3]$ for a terminal call option payoff $g(x) = \max(x - K, 0)$ for $K \in \{0.2, 0.5, 1, 1.75, 2, 2.1\}$, with parameter $\sigma = 0.3$ and linear market impact factor $\lambda = 5e^{-3}$.

the Monte-Carlo estimation obtained. We plot these value functions for strike values $K \in \{0.5, 2\}$ inside the training domain and $K \in \{0.2, 1, 2.1\}$ outside the training domain.

On these graphs we see that the estimation of the value of the value function is good and consistent with the Monte Carlo estimator for every strike, inside or outside of the training domain. The estimation of the derivative of the value function is not as good and we can see on the graphs that we get the worst results for the value of the strike closest to zero, $K = 0.2$ (Figure 16), and for values of the strike out of the training domain, $K = 1$ (Figure 17) and $K = 2.1$ (Figure 18).

A Alternative algorithms using multiple neural networks

We present below the Algorithm 7, which is the version of Algorithm 3 using two neural networks, described in Section 5.3.

Algorithm 7: Deep learning scheme for Pathwise martingale learning with 2 NN

Result: A set of optimized parameters η^*, δ^* ;

Initialize the learning rate l , the neural networks $\vartheta^\eta, \mathcal{Z}^\delta$;

Generate an \mathbb{R}^{N+1} -valued time grid $0 = t_0 < t_1 < \dots < t_N = T$ with time steps $(\Delta t_n)_{n=0, \dots, N-1}$;

Generate a batch of M starting points $X_0 \sim \mu_0$ and Brownian increments $(\Delta W_{t_n})_{n=0, \dots, N}$ in \mathbb{R}^d ;

for each batch element m do

Compute the trajectory $(x_{t_n}^m)_{n=0, \dots, N}$ through the scheme

$$x_{t_{n+1}}^m = x_{t_n}^m + b^{a^*}(t_n, x_{t_n}^m)\Delta t_n + \sigma^{a^*}(t_n, x_{t_n}^m)\Delta w_{t_n}^m,$$

from the generated starting point $x_{t_0}^m$, Brownian increments $(\Delta w_{t_n}^m)_{n=0, \dots, N-1}$ and previously trained control $a = a_{\theta^*}$;

Compute the value target $(y_T^{m, t_n})_{n=0, \dots, N}$;

end

for each epoch do

Compute, for every batch element m , the integral

$$\sum_{n=0}^{N-1} \left| y_T^{m, t_n} - \vartheta^\eta(t_n, x_{t_n}^m) - \sum_{p=n}^{N-1} (\mathcal{Z}^\delta(t_p, x_{t_p}^m))^\top \sigma^{a^*}(t_p, x_{t_p}^m) \Delta w_{t_p}^m \right|^2 \Delta t_n;$$

Compute the batch loss $\tilde{MSE}_{mar}(\eta, \delta)$;

Compute the gradient $\nabla_\eta \tilde{MSE}_{mar}(\eta, \delta)$ and $\nabla_\delta \tilde{MSE}_{mar}(\eta, \delta)$;

Update $\eta \leftarrow \eta - l \nabla_\eta \tilde{MSE}_{mar}(\eta, \delta)$, $\delta \leftarrow \delta - l \nabla_\delta \tilde{MSE}_{mar}(\eta, \delta)$;

end

Return: The set of optimized parameters η^*, δ^* ;

In the same way, the Algorithm 8 below is the version of Algorithm 4 using three neural networks described in Section 5.3.

Algorithm 8: Deep learning scheme for Pathwise differential learning with 3 NN

Result: A set of optimized parameters η^* ;

Initialize the learning rate l , the neural networks ϑ^η ;

Generate an \mathbb{R}^{N+1} -valued time grid $0 = t_0 < t_1 < \dots < t_N = T$ with time steps $(\Delta t_n)_{n=0, \dots, N-1}$;

Generate a batch of M starting points $X_0 \sim \mu_0$ and Brownian increments $(\Delta W_{t_n})_{n=0, \dots, N}$ in \mathbb{R}^d ;

for each batch element m do

 Compute the trajectory $(x_{t_n}^m)_{n=0, \dots, N}$ through the scheme

$$x_{t_{n+1}}^m = x_{t_n}^m + b^{a^*}(t_n, x_{t_n}^m) \Delta t_n + \sigma^{a^*}(t_n, x_{t_n}^m) \Delta w_{t_n}^m,$$

 from the generated starting point $x_{t_0}^m$, Brownian increments $(\Delta w_{t_n}^m)_{n=0, \dots, N-1}$ and previously trained control $a = a_{\theta^*}$;

 Compute the value and derivative targets $(y_T^{m, t_n})_{n=0, \dots, N}$ and $(z_T^{m, t_n})_{n=0, \dots, N}$;

end

for each epoch do

 Compute, for every batch element m , the integral

$$\sum_{n=0}^{N-1} \left| y_T^{m, t_n} - \vartheta^\eta(t_n, x_{t_n}^m) - \sum_{p=n}^{N-1} (D_x \vartheta^\eta(t_p, x_{t_p}^m))^\top \sigma^{a^*}(t_p, x_{t_p}^m) \Delta w_{t_p}^m \right|^2 \Delta t_n;$$

 Compute the batch loss $MSE_{mar}(\eta)$;

 Compute the gradient $\nabla_\eta MSE_{mar}(\eta)$;

 Update $\eta \leftarrow \eta - l \nabla_\eta MSE_{mar}(\eta)$;

 Compute, for every batch element m , the integral

$$\sum_{n=0}^{N-1} \left| z_T^{m, t_n} - D_x \vartheta^\eta(t_n, x_{t_n}^m) - \sum_{p=n}^{N-1} \left([D_x \sigma^{a^*}(t_p, x_{t_p}^m) \bullet_3 D_{x_{t_n}} x_{t_p}^m] \bullet_1 D_x \vartheta^\eta(t_p, x_{t_p}^m) + \sigma^{a^*}(t_p, x_{t_p}^m)^\top D_{xx} \vartheta^\eta(t_p, x_{t_p}^m) D_{x_{t_n}} x_{t_p}^m \right)^\top \Delta w_{t_p}^m \right|^2 \Delta t_n;$$

 Compute the batch loss $MSE_{dermar}(\eta)$;

 Compute the gradient $\nabla_\eta MSE_{dermar}(\eta)$;

 Update $\eta \leftarrow \eta - l \nabla_\eta MSE_{dermar}(\eta)$;

end

Return: The set of optimized parameters η^* ;

References

- [1] Chistian Beck, Sebastian Becker, Patrick Cheridito, Arnulf Jentzen, and Ariel Neufeld. Deep splitting method for parabolic PDEs. *SIAM Journal on Scientific Computing*, 43(5), 2021.
- [2] Christian Beck, Weinan E, and Arnulf Jentzen. Machine learning approximation algorithms for high-dimensional fully nonlinear partial differential equations and second-order backward stochastic differential equations. *J. Nonlinear Sci.*, 29(4):1563–1619, 08 2019.
- [3] Christian Beck, Martin Hutzenthaler, Arnulf Jentzen, and Benno Kuckuck. An overview on deep learning-based approximation methods for partial differential equations. *arXiv preprint: 2012.12348*, 2020.

- [4] James Bergstra and Yoshua Bengio. Random search for hyper-parameter optimization. *Journal of Machine Learning Research*, 13(2), 2012.
- [5] Tianping Chen and Hong Chen. Universal approximation to nonlinear operators by neural networks with arbitrary activation functions and its application to dynamical systems. *IEEE Transactions on Neural Networks*, 6(4):911–917, 1995.
- [6] Weinan E., Jiequn Han, and Arnulf Jentzen. Deep learning-based numerical methods for high dimensional parabolic partial differential equations and backward stochastic differential equations. *Commun. Math. Stat.*, 5(4):349–380, 2017.
- [7] Nicole El Karoui, Marie-Claire Quenez, and Shige Peng. Backward stochastic differential applications in finance. *Mathematical Finance*, 7(1):1–71, 1997.
- [8] Maximilien Germain, Huyên Pham, and Xavier Warin. Neural networks-based algorithms for stochastic control and PDEs in finance. *to appear in Machine learning for financial markets: a guide to contemporary practices*, 2021.
- [9] Paul Glasserman. *Monte Carlo methods in financial engineering*, volume 53. Springer Science & Business Media, 2013.
- [10] Kathrin Glau and Linus Wunderlich. The deep parametric PDE method: application to option pricing. *arXiv preprint arXiv:2012.06211*, 2020.
- [11] Emmanuel Gobet and Rémi Munos. Sensitivity analysis using Itô-Malliavin calculus and martingales, and application to stochastic optimal control. *SIAM J. Control Optim.*, 43(5):1676–1713, 2005.
- [12] Jiequn Han and Weinan E. Deep learning approximation for stochastic control problems. *Deep Reinforcement Learning Workshop, NIPS, arXiv preprint: 1611.07422*, 2016.
- [13] Jiequn Han, Arnulf Jentzen, and Weinan E. Solving high-dimensional partial differential equations using deep learning. *Proc. Natl. Acad. Sci. USA*, 115, 2017.
- [14] Brian Norsk Høge and Antoine Savine. Differential machine learning. *Available at SSRN 3591734*, 2020.
- [15] Côme Huré, Huyên Pham, Achref Bachouch, and Nicolas Langrené. Deep neural networks algorithms for stochastic control problems on finite horizon: convergence analysis. *SIAM Journal on Numerical Analysis*, 59(1):525–557, 2021.
- [16] Côme Huré, Huyên Pham, and Xavier Warin. Deep backward schemes for high-dimensional nonlinear PDEs. *Mathematics of Computation*, 89(324):1547–1579, 2020.

- [17] Shaolin Ji, Shige Peng, Ying Peng, and Xichuan Zhang. Three algorithms for solving high-dimensional fully coupled FBSDE through deep learning. *IEEE Intelligent Systems*, 35(3):71–84, 2020.
- [18] Grégoire Loeper. Option pricing with linear market impact and nonlinear Black–Scholes equations. *Annals of Applied Probability*, 28(5):2664–2726, 2018.
- [19] Francis A Longstaff and Eduardo S Schwartz. Valuing american options by simulation: a simple least-squares approach. *The review of financial studies*, 14(1):113–147, 2001.
- [20] Lu Lu, Pengzhan Jin, and George Em Karniadakis. DeepONet: Learning nonlinear operators for identifying differential equations based on the universal approximation theorem of operators. *arXiv preprint arXiv:1910.03193*, 2019.
- [21] Jin Ma and Jianfeng Zhang. Representation theorems for backward stochastic differential equations. *Annals of Applied Probability*, 12(4):1390–1418, 2002.
- [22] Balint Negyesi, Kristoffer Andersson, and Cornelis Oosterlee. The one step Malliavin scheme: new discretization of bsdes implemented with deep learning regressions. *arXiv preprint arXiv:2110.05421*, 2021.
- [23] David Nualart. *The Malliavin calculus and related topics*. Springer-Verlag, Berlin, 1995.
- [24] Nikolas Nüsken and Lorenz Richter. Interpolating between BSDEs and PINNs: deep learning for elliptic and parabolic boundary value problems. *arXiv:2112.03749*, 2021.
- [25] Huyên Pham, Xavier Warin, and Maximilien Germain. Neural networks-based backward scheme for fully nonlinear PDEs. *SN Partial Differential Equations and Applications*, 2(1):1–24, 2021.
- [26] Marc Potters, Jean-Philippe Bouchaud, and Dragan Sestovic. Hedged Monte-Carlo: low variance derivative pricing with objective probabilities. *Physica A: Statistical Mechanics and its Applications*, 289(3-4):517–525, 2001.
- [27] Philip E Protter. Stochastic differential equations. In *Stochastic integration and differential equations*, pages 249–361. Springer, 2005.
- [28] Maziar Raissi, Paris Perdikaris, and George E Karniadakis. Physics-informed neural networks: A deep learning framework for solving forward and inverse problems involving nonlinear partial differential equations. *Journal of Computational Physics*, 378:686–707, 2019.
- [29] Carl Remlinger, Joseph Mikael, and Romuald Elie. Robust operator learning to solve PDE. 2022.

- [30] Justin Sirignano and Konstantinos Spiliopoulos. Dgm: A deep learning algorithm for solving partial differential equations. *Journal of Computational Physics*, 375:1339–1364, 2018.
- [31] H Mete Soner, Nizar Touzi, and Jianfeng Zhang. Dual formulation of second order target problems. *The Annals of Applied Probability*, 23(1):308–347, 2013.
- [32] Rupesh K Srivastava, Klaus Greff, and Jürgen Schmidhuber. Training very deep networks. *Advances in neural information processing systems*, 28, 2015.
- [33] Remco van der Meer, Cornelis W Oosterlee, and Anastasia Borovykh. Optimally weighted loss functions for solving PDEs with neural networks. *Journal of Computational and Applied Mathematics*, page 113887, 2021.
- [34] Marc Sabate Vidales, David Siska, and Lukasz Szpruch. Unbiased deep solvers for parametric PDEs. *arXiv preprint arXiv:1810.05094*, 2018.